

Bacterial and eukaryotic intact polar lipids point to *in situ* production as a key source of labile organic matter in hadal surface sediment of the Atacama Trench

Edgart Flores^{1,2,3*}, Sebastian I. Cantarero⁴, Paula Ruiz-Fernández^{1,2,3}, Nadia Dildar⁴,
Matthias Zabel⁵, Osvaldo Ulloa^{2,3} and Julio Sepúlveda^{3,4*}

¹Programa de Postgrado en Oceanografía, Departamento de Oceanografía, Facultad de Ciencias Naturales y Oceanográficas, Universidad de Concepción, Concepción, Chile

²Departamento de Oceanografía, Universidad de Concepción, Casilla 160-C, Concepción, Chile

³Millennium Institute of Oceanography, Universidad de Concepción, Concepción, Chile

⁴Department of Geological Sciences and Institute of Arctic and Alpine Research, University of Colorado Boulder, Boulder, CO 80309, USA

⁵MARUM – Center for Marine Environmental Sciences & Department of Geosciences, Univ. of Bremen, D-28334, Bremen, Germany

*Correspondence to: Edgart Flores (edgart.flores@imo-chile.cl), Julio Sepúlveda (jsepulveda@colorado.edu)

Abstract. Elevated organic matter (OM) concentrations are found in hadal surface sediments relative to the surrounding abyssal seabed. However, the origin of this biological material remains elusive. Here, we report on the composition and distribution of cellular membrane intact polar lipids (IPLs) extracted from surface sediments around the deepest points of the Atacama Trench and adjacent bathyal margin to assess and constrain the sources of labile OM in the hadal seabed. Multiscale bootstrap resampling of IPLs' structural diversity and abundance indicates distinct lipid signatures in the sediments of the Atacama Trench that are more closely related to those found in bathyal sediments than to those previously reported for the upper ocean water column in the region. Whereas the overall number of unique IPL structures in hadal sediments contributes a small fraction of the total IPL pool, we also report a high contribution of phospholipids with mono- and di-unsaturated fatty acids that are not associated with photoautotrophic sources, and that resemble traits of physiological adaptation to high pressure and low temperature. Our results indicate that IPLs in hadal sediments of the Atacama Trench predominantly derive from *in situ* microbial production and biomass, whereas the export of the most labile lipid component of the OM pool from the euphotic zone and the overlying oxygen minimum zone is neglectable. While other OM sources such as the downslope and/or lateral transport of labile OM cannot be ruled out and remain to be studied, they are likely less important in view of the lability of ester-bond IPLs. Our results contribute to the understanding of the mechanisms that control the delivery of labile OM to this extreme deep-sea ecosystem. Furthermore, they provide insights into some potential physiological adaptation of the *in situ* microbial community to high pressure and low temperature through lipid remodeling.

1. Introduction

The deep ocean has been classically considered a vast "biological desert" (Danovaro et al., 2003) due to the attenuation of organic matter (OM) fluxes with increasing depth (Wakeham et al., 1984; Martin et al., 1987; Hedges et al., 2001; Rex et al., 2006). However, hadal trenches (~6,000-11,000 m below sea level) contradict this paradigm (Danovaro et al., 2003; Glud et al., 2013; Leduc et al., 2016; Wenzhöfer et al., 2016; Luo et al., 2017),

as they act as depocenters of OM (Jahnke and Jahnke, 2000) and hotspots for microbial activity (Glud et al., 2013; Wenzhöfer et al., 2016; Liu et al., 2019). Indeed, OM availability is considered the major factor controlling the abundance, biomass, and diversity of life in the deep ocean (Danovaro et al., 2003; Ichino et al., 2015), whereas hydrostatic pressure appears to be an important and additional factor controlling biological activity in hadal trench systems (Jamieson et al., 2010; Tamburini et al., 2013). However, our understanding of the composition, sources, and lability of OM in marine trenches remains limited. According to Xu et al. (2018), the main sources of OM to the hadal zone include: (1) the vertical sinking of particulate OM (POM); (2) the carrion falls of dead bodies; (3) inputs of terrestrial OM; (4) downslope transport of OM from continental slopes; and (5) *in situ* chemosynthetic production associated with cold seeps or hydrothermal vents. Several studies have highlighted the importance of POM sinking mainly from the euphotic zone (Stockton and DeLaca, 1982; Angel, 1984; Gooday et al., 2010). In fact, POM fluxes measured at 4,000 m in the North Pacific Subtropical Gyre Ocean reveal that a seasonal export pulse can exceed the mean annual flux by ~150% (Poff et al., 2021). However, it is unknown whether such pulses reach the hadal sediments (6,000-11,000 m). Downslope transport, on the other hand, can be facilitated by trench topography and gravity (Jahnke et al., 1990; Fischer et al., 2009; Inthorn et al., 2006; Ichino et al., 2015) and/or by earthquakes (Glud et al., 2013; Kioka et al., 2019), as recently reported in the Japan Trench (Schwestermann et al., 2021). Independent of the main sources of OM, which are spatially and temporally variable, the channeling of allochthonous OM to the hadal zone should be facilitated by the characteristic V-shape cross-section of trenches, unique tectonic position in the ocean, and the physiography of the canyons that connect to coast systems (Itou et al., 2000; Itoh et al., 2011; Bao et al., 2018). Additionally, autochthonous OM sources include *in situ* microbial biomass production (Smith, 2012; Nunoura et al., 2016; Ta et al., 2019; Hand et al., 2020), although their overall contribution as a secondary input to carbon budgets and energy flow in these systems remains poorly constrained (Grabowski et al., 2019). The spatial variations in community structure seen in benthic prokaryotic populations in hadal regions such as the Mariana, Japan, and Izu-Ogasawara trenches have been attributed to the variability of biogeochemical conditions, mainly nitrate and oxygen availability (Hiraoka et al., 2020), with benthic oxygen consumption exhibiting heterogeneity (Glud et al., 2021). Recent metagenomic data has revealed the presence of abundant heterotrophic microorganisms in sediments of the Challenger Deep (Nunoura et al., 2018), which are likely fueled by the endogenous recycling of available OM (Nunoura et al., 2015; Tarn et al., 2016). Furthermore, the abundance of prokaryotes in hadal depths can be influenced by dynamic depositional conditions (Schauberger et al., 2021), which in turn may be influenced by the intensity of propagating internal tides (Turnewitsch et al., 2014). All these factors likely alter the deposition, distribution, and composition of OM present in trench sediments.

An alternative approach to study microbial processes and the contribution of autochthonous OM is the use of cell membrane intact polar lipids (IPLs), which although less specific than genomic markers, allow for more quantitative estimates of microbial biomass in nature (e.g., Lipp et al., 2008; Schubotz et al., 2009; Cantarero et al., 2020). IPLs are composed of a polar head group typically attached to a glycerol backbone from which aliphatic chains are attached via ester and/or ether bonds (Sturt et al., 2004). Their structural diversity is given by the modifications found in the different components of their chemical structure (e.g., polar head groups can be comprised of phosphorous, nitrogen, sulfur, sugars, and amino acids), whereas aliphatic chains (alkyl or isoprenoidal) can vary in their length (number of carbon atoms), and their degree of unsaturation, methylation, hydroxylation, and cyclization (Van Mooy and Fredricks, 2010; Brandsma et al., 2011; Schubotz et al., 2013). In

bacteria and eukarya, alkyl chains are most commonly linked via an ester bond to the sn-glycerol-3-phosphate backbone (Koga and Morii, 2007), although some bacteria are known to produce di- and tetraether lipids (Weijers et al., 2007). The variability of membrane chemical structures underlies the adaptability of microbial lifestyles to changing environmental conditions such as nutrients, temperature, oxygen, pH, and pressure (DeLong and Yayanos, 1985; Somero, 1992; Van Mooy et al., 2009; Carini et al., 2015; Sebastián et al., 2016; Siliakus et al., 2017; Boyer et al., 2020). Furthermore, since eukaryotic and bacterial ester-bond IPLs are more labile than ether-bond counterparts (Logemann et al., 2011), they are suitable biomarkers to evaluate sources of labile OM in marine environments.

IPLs have been previously used as microbial markers in diverse marine settings, such as along strong redox gradients in the Black Sea (Schubotz et al., 2009b) and the oxygen minimum zones (OMZs) of the eastern tropical Pacific (Schubotz et al., 2018a; Cantarero et al., 2020) and the Arabian Sea (Pitcher, 2011), as well as in surface open ocean waters of the eastern south Pacific (Van Mooy and Fredricks, 2010), the northwestern Atlantic (Popendorf et al., 2011b), and the Mediterranean Sea (Popendorf et al., 2011a), to name a few. Their utility as markers of microbial diversity and processes has also been tested in marine sediments (Liu et al., 2011, 2012; Sturt et al., 2004), such as along the Peru Margin, Equatorial Pacific, Hydrate Ridge, and Juan de Fuca Ridge (Lipp and Hinrichs, 2009a) and in subsurface sediment layers from the Peru Margin (Biddle et al., 2006). However, to the best of our knowledge, no IPL studies have been reported for sediments of hadal trenches.

In this study, we investigate the chemical diversity and abundance of microbial IPLs as markers of one the most labile molecular fractions of OM in sediments of the deepest points of the Atacama Trench, and compare them to IPL stocks in bathyal surface sediments (~500-1,200 m) and the overlying 700 m of the water column (Cantarero et al., 2020). More specifically, we evaluate possible IPL provenance (*in situ* vs. allochthonous production), and the presence of unique IPL signatures of the *in situ* microbial community as well as evidence for molecular adaptations to the extreme conditions of the hadal region.

2. Material and Methods

2.1 Study areas and sampling

The Atacama Trench is located in the eastern tropical South Pacific (ETSP) along the Peru-Chile margin, and it underlies the eutrophic and highly productive Humboldt Current System (Angel, 1982; Ahumada, 1989), which includes the fourth largest (by volume) oxygen minimum zone (OMZ) in the world (Schneider et al., 2006). In this area, while there is minimal river runoff (Houston, 2006), winds can transfer dust from the adjacent continental desert (Angel, 1982). With an extension of ~5,900 km, the Atacama Trench is the world's largest trench (Sabbatini et al., 2002), whereas it is geographically isolated from other trenches in the Pacific Ocean.

In this study, we investigated the diversity and abundance of bacterial and eukaryotic IPLs in a total of 9 hadal surface (0-1 cm) and subsurface (1-2 and 2-3 cm) sediments (3 sites between 7,734 and 8,063 m water depth) collected during the HADES-SO261 cruise (March to April 2018) onboard the RV *Sonne* (Wenzhöfer, 2019), and 7 bathyal surface sediments (7 sites; 529-1200 m water depth) collected during the ChiMeBo-SO211 cruise

(November 2-29, 2010) onboard the RV *Sonne* (Matys et al., 2017) (Table 1; Fig. 1). We compare our results against IPL results from the overlying water column (0-700 m) recently reported in Cantarero et al. (2020).

Table 1. Sampling stations from the Hades, ChiMeBo, and LowpHOX-2 expeditions.

Cruise-RV	Device	Enviroment	Station	Environmental samples	Sampling depth (m)	Latitude (°S)	Longitude (°W)	Date	Reference
HADES SONNE SO-261	Multi-corer (MUC)	Hadal sediments	A10	Hadal sediments (0-1, 1-2 and 2-3 cm)	7734	20.32	71.29	26/03/2018	This study
			A5	Hadal sediments (0-1, 1-2 and 2-3 cm)	7890	23.81	71.37	11/03/2018	
			A4	Hadal sediments (0-1, 1-2 and 2-3 cm)	8063	23.36	71.34	14/03/2018	
ChiMeBo SONNE SO-211	Multi-corer (MUC)	Bathyal Sediments	B12	Upper bathyal sediment (0-1 cm)	529	23.59	70.67	02-29/11/2010	This study
			B08	Upper bathyal sediment (0-1 cm)	539	25.2	70.68	02-29/11/2010	
			B22	Upper bathyal sediment (0-1 cm)	545	27.29	71.05	02-29/11/2010	
			B07	Lower bathyal sediment (0-1 cm)	920	25.07	70.66	02-29/11/2010	
			B05	Lower bathyal sediment (0-1 cm)	957	27.5	71.13	02-29/11/2010	
			B11	Lower bathyal sediment (0-1 cm)	1113	23.85	70.65	02-29/11/2010	
			B04	Lower bathyal sediment (0-1 cm)	1200	27.45	71.16	02-29/11/2010	
LowpHOX-2 Cabo de Hornos	Rosette (Niskin bottles)	Water column	T3/T5	Chlorophyll maximum (0.3-2.7 µm)	9-10	20.07/20.03	70.36/70.89	04-06/02/2018	Cantarero et al., 2020
			T3/T5	Upper chemocline (0.3-2.7 µm)	25-28	20.07/20.03	70.36/70.89	04-06/02/2018	
			T3/T5	Lower chemocline (0.3-2.7 µm)	35-45	20.07/20.03	70.36/70.89	04-06/02/2018	
			T3/T5	Upper OMZ (0.3-2.7 µm)	55-60	20.07/20.03	70.36/70.89	04-06/02/2018	
			T3/T5	Core OMZ (0.3-2.7 µm)	250	20.07/20.03	70.36/70.89	04-06/02/2018	
			T3/T5	Mesopelagic zone (0.3-2.7 µm)	750	20.07/20.03	70.36/70.89	04-06/02/2018	

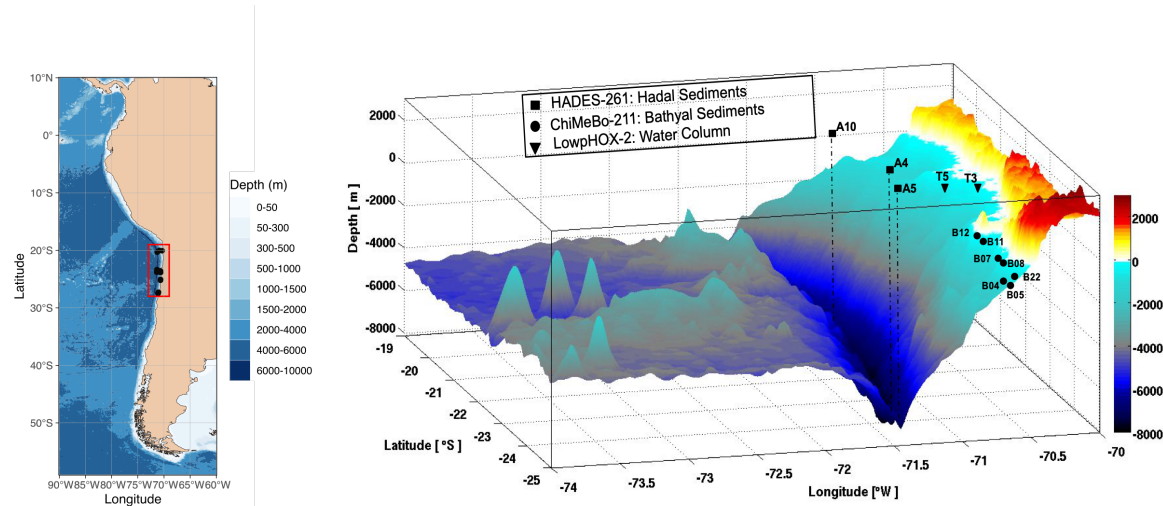


Figure 1. Three-dimensional map of the Atacama Trench showing the sampling locations of this study. The black squares indicate the hadal sediment sampling stations, the black circles indicate the bathyal sediment sampling stations from Matys et al. (2017), and the black triangles indicate water column sampling stations from Cantarero et al. (2020).

Sediment samples were collected using a multi-corer (MUC) equipped with twelve 60-cm-long acrylic tubes (6-10 cm diameter for bathyal sediments and 9.5 cm diameter for hadal sediments). During the HADES expedition, an autonomous lander equipped with a Seabird SBE-19 plus CTD and 2 Niskin bottles (30 L) was used to obtain hydrographic data down to ~7850 m. Hadal sediments from the HADES-SO261 cruise were stored at 4°C until they were extruded and subsampled onboard at 1-cm resolution, and then kept frozen at -20°C until their processing in the laboratory. Further information about sample collection of bathyal and hadal sediments during the ChiMeBo-SO211 and HADES-SO261 cruises can be found in Matys et al. (2017) and Wenzhöfer et al., (2019), respectively.

We compare our IPL results from surface sediment in the hadal and bathyal regions against samples from the overlying water column from the LowPhOx-2 cruise recently reported by Cantarero et al. (2020). This includes size-fractionated suspended OM (0.3-2.7 μm and 2.7-53 μm) at two stations and from six water depths that are representative of the dominant biogeochemical zonation associated with the OMZ of this region: chlorophyll maximum (~10 m), upper chemocline (~25 m), lower chemocline (~45 m), upper OMZ (~60 m), core OMZ (~250 m), and mesopelagic zone (~750 m) (See Table 1 and Cantarero et al., 2020 for further details).

2.2 Analytical methods

2.2.1 Lipid extraction

All samples were processed, extracted, and analyzed in the Organic Geochemistry Laboratory at the University of Colorado Boulder. Sediment samples were freeze dried before extraction. Approximately 1-2 grams of dry sediment was placed in a combusted glass centrifuge tube and extracted using a modified version (Wörmer et al., 2013) of the Bligh and Dyer Extraction method (Bligh and Dyer, 1959) as detailed in Cantarero et al. (2020). Briefly, before extraction, we added 1 μg of C16 PAF ($\text{C}_{26}\text{H}_{54}\text{NO}_7\text{P}$) to each sample as an internal standard. Samples were sequentially extracted using dichloromethane:MeOH:phosphate buffer (1:2:0.8 v:v:v; 2x), dichloromethane:MeOH:trichloroacetic buffer (1:2:0.8 v:v:v; 2x) and dichloromethane:MeOH (1:5 v:v; 1x). After each addition, samples were vortexed for 30 seconds, sonicated for 10 minutes, and then centrifuged for 5 minutes at 2000 rpm. Each extraction was then transferred to a separatory funnel where a total lipid extract (TLE) was combined and then concentrated under a gentle N_2 stream. Before analysis, the TLEs were resuspended in dichloromethane:methanol (9:1) v/v and filtered through a 0.45 μm polytetrafluoroethylene (PTFE) syringe filter. The processing and extraction of bathyal sediments from the ChiMeBo-SO211 cruise and water column samples from the LowpHOx-2 cruise has been reported by Matys et al. (2017) and Cantarero et al. (2020), respectively. TLEs were transferred into 2 ml vials with 200 μl inserts, and dissolved in 100 μl of dichloromethane:MeOH [9:1, v:v].

2.2.2 IPL analysis

IPL were analyzed according to Wörmer et al. (2013) and as described in Cantarero et al. (2020) using a Thermo Scientific Ultimate 3000 High Performance Liquid Chromatograph (HPLC) coupled to a Q Exactive Focus Orbitrap-Quadrupole High Resolution Mass Spectrometer (HPLC-HRMS) via electrospray ionization (ESI). The HPLC program comprised a flow rate of 0.4 mL/min using a mixture of two mobile phases: mixture A consisted of acetonitrile:dichloromethane (75:25, v:v) with 0.01% formic acid and 0.01% NH_4OH ; mixture B consisted of methanol:water (50:50, v:v) with 0.4% formic acid and 0.4% NH_4OH . We used a linear gradient as follows: 1% B (0–2.5 min), 5% (4 min), 25% B (22.5 min), 40% B (26.5 min–27.5 min), and the HPLC column was kept at 40 $^\circ\text{C}$. Samples were injected (10 μl) dissolved in dichloromethane:methanol (9:1, v:v). IPLs were separated using a Waters Acquity BEH Amide column (2.1 \times 150 mm; 1.7 μm particle size) that enables class-specific separation based on their hydrophilic head group (Wörmer et al., 2013).

ESI settings comprised: sheath gas (N₂) pressure 35 (arbitrary units), auxiliary gas (N₂) pressure 13 (arbitrary units), spray voltage 3.5 kV (positive ion ESI), capillary temperature 265°C, S-Lens RF level 55 (arbitrary units). The instrument was calibrated for mass resolution and accuracy using the Thermo Scientific Pierce LTQ Velos ESI Positive Ion Calibration Solution (containing a mixture of caffeine, MRFA, Ultramark 1621, and N-butylamine in an acetonitrile/methanol/acetic acid solution).

IPLs were identified on positive ionization mode, on both full scan and data depended MS², based on their molecular weights as either protonated (M + H)⁺ or ammonium (M + NH₄)⁺ adducts compounds, fragmentation patterns, and retention times, and as compared against relevant literature (Sturt et al., 2004; Schubotz et al., 2009a; Wakeham et al., 2012) and the internal database of the Organic Geochemistry Lab at CU Boulder.

The peak areas of individual IPLs were integrated using the Thermo Fisher Scientific TraceFinder software using extracted ion chromatograms of their characteristic molecular ions. IPL abundances were determined with a combination of an internal standard (C₁₆PAF, Avanti Lipids) and an external calibration to a linear regression between peak areas and known concentrations of an IPL cocktail comprised of 17 different IPL classes across a 5-point dilution series (0.001–2.5 ng/μl) (see Cantarero et al., 2020). Deuterated standards (Avanti Lipids: d7-PC, d7-PG, d7-PE and d9-DGTS) were used to correct for potential matrix effects on ionization efficiency. Despite the limited number of available deuterated standards, on average, we observed that the matrix effect accounts for a loss of ~7±0.6% in ionization efficiency. Therefore, it is reasonable to assume a similar loss for other IPL classes, although this remains to be tested in future studies. We highlight the importance of using as many IPLs classes as possible to account for both differences in ionization efficiency and matrix effect when performing IPL quantification in environmental samples. The relative response factors followed the order: MGDG > DGTS > DGTA > PDME > PME > PG > PC > PE > SQDG > DGCC > DGDG. Lipids classes were grouped into phospholipids (PG; phosphatidylglycerol, PE; phosphatidylethanolamine, PC; phosphatidylcholine, and PME/PDME; Phosphatidyl(di)methylethanolamine), glycolipids (MG; Monoglycosyldiacylglycerol, DG; Diglycosyldiacylglycerol, and SQDG; Sulfoquinovosyldiacylglycerol), Betaine lipids (DGTA; Diacylglyceryl hydroxymethyl-trimethyl-β-alanine, DGTS; Diacylglyceryl trimethylhomoserine, and DGCC; Diacylglycerylcarboxy-N-hydroxymethyl-choline) and Other lipids (Gly-Cer; Glycosidic ceramides, PI; phosphatidylinositol, and OL; Ornithine lipids). In addition, we use DAG to designate a diacylglycerol and AEG to designate an acyletherglycerol, and we describe short- and long-chains to refer to combined alkyl chains of C₂₈₋₃₆ and C₃₆₋₄₄, respectively (Rêzanka et al., 2009; Schubotz et al., 2009a; Brandsma, et al., 2011).

2.3 Statistical analyses

We used the Bray–Curtis similarity coefficient (Mirzaei et al., 2008) to produce hierarchical clustering of the abundance of classes and molecules of IPLs, two types of p-values were available: approximately unbiased (AU) p-value and bootstrap probability (BP) value with the number of bootstrap replications of 10,000 (Suzuki and Shimodaira, 2006). We performed non-metric Multidimensional Scaling (NMDS) (Warton et al., 2012) to examine the dissimilarity between the IPLs in each sample. The calculated distances to group centroids were based on Bray-Curtis dissimilarity from IPLs abundances matrix, and the significance of the associations was determined

by 999 random permutations. Significance tests of the multivariate dissimilarity between groups were made using Analysis of Similarity (ANOSIM), where complete separation and no separation among groups is suggested by $R = 1$ and $R = 0$, respectively (Clarke and Gorley, 2015). Statistical differences in the numbers of carbon atoms and double bonds were identified by ANOVA and Tukey's HSD (honestly significant difference) post hoc test. We used similarity of percentage (SIMPER) analysis to identify the percentage contributions of IPLs which accounted for > 90% of the similarity within each cluster. The multivariate statistical analyses, as well as other statistical analyses were calculated using the Vegan package (Oksanen et al., 2013) of open-source software R version 3.6.2 within the ggplots package (Warnes et al., 2015).

3. Results

3.1 Hydrographic conditions

A physical-chemical characterization of the water column during the ChiMeBo-SO211, LowpHOx-2, and HADES-SO261 cruises has been reported in Matys et al. (2017), Cantarero et al. (2020) and Vargas et al. (2021), and Fernández-Urruzola et al. (2021), respectively. Briefly, the potential temperature-salinity-dissolved oxygen (θ -s- O_2) diagrams revealed an oxygenated and well-mixed water mass occupying the deeper parts of the Atacama Trench (Fig. S1). However, the upper 1000 m shows variability in temperature (12-23 °C), salinity (34.4-34.8 psu) and oxygen (0.5-267 μ M). More stable physical-chemical conditions are apparent in the mesopelagic and bathypelagic zone of the Atacama Trench between 1000 and 4000 m, (temperature \sim 2.3 °C, salinity \sim 34.6 psu, oxygen \sim 120.6 μ M). Below 4000 m, average conditions were characterized by a potential temperature \sim 1.8 °C, salinity \sim 34.7 psu, and oxygen \sim 143 μ M (Fig. S1).

3.2 IPLs in surface sediments of the Atacama trench

3.2.1 Distribution of IPL classes by polar head groups

The 16 sediment samples from bathyal and hadal regions statistically grouped into four clusters based on their dominant polar head group classes (Fig. 2, chemical structures in Fig. S2). Clusters 1 and 2 had approximately unbiased (AU) p-values of 91% and 88%, respectively. Cluster 3 had the highest AU p-value of \geq 97%, whereas Cluster 4 had the lowest AU p-value of 61%. The cluster analysis revealed a degree of spatial heterogeneity between bathyal and hadal depths and between the top three centimeters of hadal sediments, which results in the lack of a clear separation between hadal and bathyal environments. In addition, the 0-1 cm hadal sediments at A4 station were un-clustered, consistent with a distinct distribution pattern of IPL classes. Cluster 1, composed of only hadal samples from three different stations and depths, included phospholipids as the most abundant IPL class (Fig. 2). Clusters 2, 3 and 4, composed of mixed bathyal and hadal samples, were mostly differentiated by changes in the relative abundances of non-phosphorous IPLs including betaine classes. The un-clustered sample was characterized by the lowest relative abundance of phospholipids and the highest relative abundance of betaine lipids (especially DGCC).

297 AR, PE 32:1, PG-DAG-36:2, DGCC 27:0 and 26:0, and PC-DAG-33:2 contributing 38.1% of it (Table 2). The
 298 total dissimilarity between Clusters 1 and 4 was 62.5%, with DGCC 42:6, PC-DAG-30:2, PE 32:1, PC-DAG-
 299 35:0, PG-DAG-36:2, PC-DAG-33:2, and DGCC 27:0 contributing 37.62% of it (Table 2).

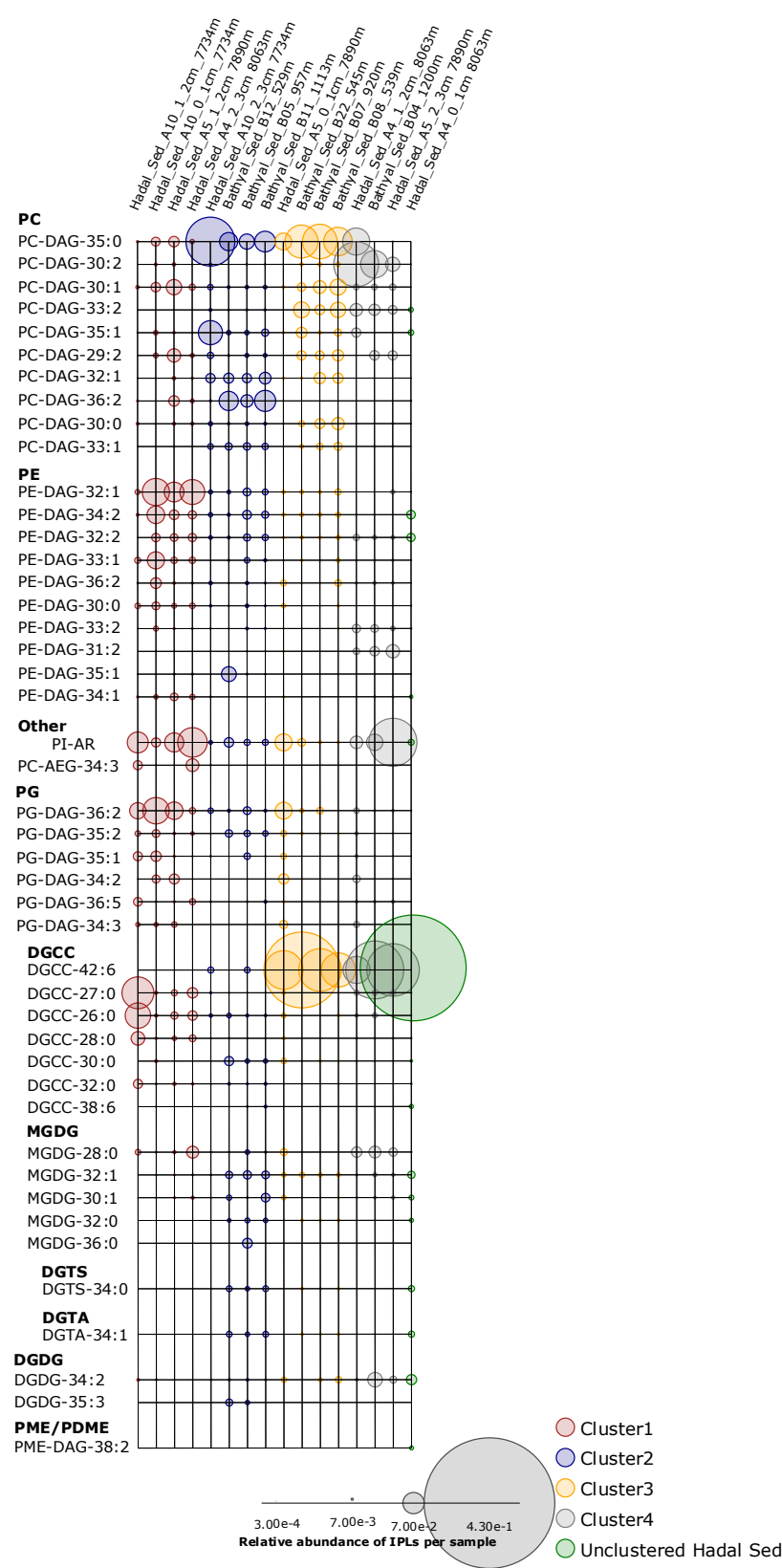


Figure 3. Relative abundance of individual IPLs contributing most of the dissimilarity between the 4 clusters shown in Fig. 2. Sampling stations are organized left to right and are shown using the same order from hierarchical clusters in Fig. 2, whereas IPL classes are organized from top to bottom. The circle size is proportional to the relative abundance of IPLs in each sample (bottom panel).

Table 2. Similarity percentage (SIMPER) analysis. The average abundance and contribution of IPLs that explain the main differences among the sediment samples is based on the hierarchical clusters shown in Fig. 2.

Group Cluster 1						Groups Cluster 1 & Cluster 2						
Cluster 1: Average Similarity = 59.53						Average dissimilarity = 59.17						
IPLs	Average Cluster 1	Average Similarity	Similarity/S D	Contribution (%)	Cumulative (%)	IPLs	Average Cluster 1	Average Cluster 2	Average Dissimilarity	Dissimilarit y/SD	Contribution (%)	Cumulative (%)
PI-AR	0.06	4.76	2.46	7.99	7.99	PC-DAG-35:0	0.02	0.08	3.18	1.34	5.37	5.37
PE-DAG-32:1	0.06	4.37	1.45	7.34	15.33	PE-DAG-32:1	0.06	0.02	2.35	1.73	3.98	9.35
PG-DAG-36:2	0.05	3.79	2	6.36	21.69	PI-AR	0.06	0.02	2.21	1.74	3.73	13.08
PE-DAG-33:1	0.03	2.06	33.49	3.45	25.14	PG-DAG-36:2	0.05	0.02	1.98	1.64	3.35	16.43
PE-DAG-34:2	0.03	1.89	1.74	3.17	28.31	DGCC-27:0	0.04	0	1.93	1	3.26	19.69
DGCC-26:0	0.04	1.84	2.04	3.09	31.4	PC-DAG-36:2	0.01	0.05	1.79	1.57	3.02	22.71
PC-DAG-30:1	0.03	1.76	2.21	2.96	34.36	PC-DAG-34:1	0	0.04	1.79	1.03	3.02	25.73
DGCC-27:0	0.04	1.74	1.8	2.93	37.3	PC-DAG-32:1	0.01	0.03	1.36	5.58	2.3	28.03
PE-DAG-30:0	0.02	1.7	13.1	2.86	40.15	DGCC-26:0	0.04	0.01	1.34	0.95	2.27	30.3
PE-DAG-32:2	0.02	1.39	1.07	2.34	42.49	PC-DAG-35:1	0.01	0.03	1.27	0.9	2.15	32.45
PC-DAG-35:0	0.02	1.31	1.52	2.2	44.69	PE-DAG-33:1	0.03	0.01	1.02	1.2	1.73	34.18
DGCC-28:0	0.02	1.22	1.96	2.05	46.74	PC-DAG-33:1	0	0.02	0.96	7.61	1.63	35.8
PC-DAG-26:0	0.02	1.18	1.46	1.99	48.73	DGCC-28:0	0.02	0	0.93	1.28	1.57	37.37
PC-DAG-28:0	0.02	1.14	1.59	1.91	50.63	PC-AEG-34:3	0.02	0	0.9	1.03	1.52	38.89
Group Cluster 2						PE-DAG-34:2	0.03	0.02	0.88	1.2	1.49	40.38
Cluster 2: Average Similarity = 58.79						MGDG-32:1	0	0.02	0.83	1.81	1.4	41.78
IPLs	Average Cluster 2	Average Similarity	Similarity/S D	Contribution (%)	Cumulative (%)	PC-DAG-30:1	0.03	0.01	0.83	1.15	1.4	43.18
PC-DAG-35:0	0.08	5.63	7.54	9.58	9.58	PG-DAG-34:2	0.02	0	0.77	1.05	1.3	44.48
PC-DAG-32:1	0.03	3.12	31.24	5.3	14.88	PC-DAG-33:0	0.02	0	0.76	1.11	1.29	45.77
PC-DAG-36:2	0.05	2.74	1.13	4.67	19.55	PG-DAG-35:1	0.02	0.01	0.74	1.22	1.26	47.03
PC-DAG-33:1	0.02	2.04	10.17	3.46	23.01	PE-DAG-34:1	0.02	0	0.74	2.06	1.25	48.27
PC-DAG-35:1	0.03	1.63	4.48	2.77	25.78	PC-DAG-26:0	0.02	0	0.72	1.74	1.21	49.48
PI-AR	0.02	1.61	3.9	2.74	28.53	DGCC-30:0	0	0.01	0.68	1.32	1.15	50.64
MGDG-32:1	0.02	1.44	1.35	2.45	30.98	Groups Cluster 1 & Cluster 3						
PE-DAG-32:1	0.02	1.38	5.03	2.35	33.33	Average dissimilarity = 60.69						
PE-DAG-34:2	0.02	1.38	2.75	2.35	35.68	IPLs	Average Cluster 1	Average Cluster 3	Average Dissimilarity	Dissimilarit y/SD	Contribution (%)	Cumulative (%)
PE-DAG-32:2	0.02	1.22	2.79	2.08	37.76	DGCC-42:6	0	0.16	8.02	3.2	13.21	13.21
PC-DAG-32:0	0.01	1.14	5.69	1.94	39.69	PC-DAG-35:0	0.02	0.08	3.05	1.87	5.02	18.23
PG-DAG-36:2	0.02	1.1	3.23	1.87	41.57	PI-AR	0.06	0.05	2.66	1.6	4.39	22.62
PG-DAG-35:2	0.02	1.09	1.23	1.86	43.43	PE-DAG-32:1	0.06	0.01	2.49	1.74	4.1	26.72
PC-DAG-34:1	0.04	1.06	0.41	1.8	45.23	PG-DAG-36:2	0.05	0.02	1.9	1.49	3.14	29.86
PC-DAG-30:1	0.01	1.05	7.23	1.79	47.02	DGCC-27:0	0.04	0.01	1.84	0.97	3.03	32.89
PC-DAG-32:2	0.01	0.95	11.7	1.61	48.64	DGCC-26:0	0.04	0.01	1.59	1.12	2.62	35.52
PC-DAG-29:2	0.01	0.95	2.69	1.61	50.25	PC-DAG-33:2	0	0.03	1.58	1.7	2.61	38.12
Group Cluster 3						PE-DAG-34:2	0.03	0.01	1.13	1.35	1.86	39.98
Cluster 3: Average Similarity = 57.31						PE-DAG-33:1	0.03	0.01	1.07	1.33	1.76	41.75
IPLs	Average Cluster 3	Average Similarity	Similarity/S D	Contribution (%)	Cumulative (%)	PC-AEG-34:3	0.02	0	0.95	1.08	1.57	43.31
DGCC-42:6	0.16	12.84	6.72	22.4	22.4	PC-DAG-29:2	0.02	0.03	0.95	1.88	1.56	44.87
PC-DAG-35:0	0.08	4.78	1.14	8.33	30.74	DGCC-28:0	0.02	0	0.9	1.25	1.49	46.36
PC-DAG-33:2	0.03	2.07	1.19	3.61	34.35	PC-DAG-30:1	0.03	0.03	0.87	1.35	1.43	47.79
PC-DAG-30:1	0.03	1.96	1.82	3.42	37.77	PE-DAG-33:0	0.02	0	0.76	1.07	1.26	49.05
PC-DAG-29:2	0.03	1.79	1.2	3.12	40.89	PG-DAG-34:2	0.02	0.01	0.76	1.1	1.26	50.3
PI-AR	0.05	1.69	1.09	2.95	43.84	Groups Cluster 1 & Cluster 4						
MGDG-32:1	0.01	1.22	7.66	2.14	45.98	Average dissimilarity = 62.47						
PE-DAG-32:1	0.01	1.18	10.45	2.05	48.03	IPLs	Average Cluster 1	Average Cluster 4	Average Dissimilarity	Dissimilarit y/SD	Contribution (%)	Cumulative (%)
PC-DAG-30:0	0.02	1.13	1.22	1.97	50	DGCC-42:6	0	0.14	6.99	2.57	11.19	11.19
Group Cluster 4						PC-DAG-30:2	0.01	0.12	5.66	3.64	9.06	20.24
Cluster 4: Average Similarity = 63.64						PE-DAG-32:1	0.06	0	3.17	2.09	5.07	25.31
IPLs	Average Cluster 2	Average Similarity	Similarity/S D	Contribution (%)	Cumulative (%)	PC-DAG-35:0	0.02	0.04	2.22	1.6	3.55	28.86
PC-DAG-30:2	0.12	9.04	14.21	14.21	14.21	PG-DAG-36:2	0.05	0.01	2.12	1.64	3.4	32.27
DGCC-42:6	0.14	8.91	13.99	28.2	28.2	PC-DAG-33:2	0	0.04	1.9	15.16	3.04	35.3
PI-AR	0.05	4.14	6.5	34.71	34.71	DGCC-27:0	0.04	0.02	1.45	0.78	2.32	37.62
PC-DAG-33:2	0.04	3.71	5.83	40.54	40.54	PE-DAG-34:2	0.03	0	1.35	1.44	2.16	39.78
MGDG-28:0	0.04	3.44	5.41	45.95	45.95	PI-AR	0.06	0.05	1.3	1.6	2.08	41.86
PE-DAG-33:2	0.03	2.52	3.97	49.92	49.92	DGCC-26:0	0.04	0.01	1.26	0.89	2.02	43.88
PE-DAG-31:2	0.03	2.14	3.37	53.28	53.28	DGDG-34:2	0	0.03	1.25	1.17	2	45.88
						PE-DAG-31:2	0	0.03	1.21	4.58	1.93	47.81
						PE-DAG-33:1	0.03	0.01	1.2	1.46	1.92	49.73
						PE-DAG-33:3	0	0.02	1.16	4.61	1.86	51.59

3.3 Distribution of alkyl chains based on length and degree of unsaturation

The difference in the total number of acyl carbon atoms in both alkyl chains, rather than in individual fatty acids, and in the number of acyl double bonds within each cluster is shown in Fig. 4. Statistical differences of IPLs classes within each cluster was obtained through a Tukey HSD post-hoc test at a significant level of $p < 0.05$ (Fig. 4a, b). The average number of carbon atoms in the diglyceride moieties of IPLs in the Cluster 1 presented that DGCC, MGDG, Others, PC, and PG were all distinct from one another ($n = 283$; $P < 0.05$; Fig. 4a). PG and Others were characterized by relatively long alkyl chains (35-36 C atoms, respectively) and DGCC for shorter alkyl chains (32 C atoms). In general, Cluster 1 exhibited a wide range of chain lengths among DAGs (28-36 C atoms). Cluster 2 showed a narrower range than Cluster 1 (30-36 C atoms). This cluster also displayed no statistical difference ($p > 0.05$) among IPL classes (Fig. 4a), following pairwise comparisons with Tukey's HSD post-hoc test, despite the wide range of DGCC structures. Cluster 3, while it exhibited low variability in betaine lipids, it also revealed the highest number of carbon atoms in DGCCs (42). On the contrary, Cluster 4 presented high variability in DGCCs, which did not exceed 42 carbon atoms. Within the phospholipid class, PG showed the highest number of carbon atoms in all clusters, the mean we observed was 34 carbon atoms and a range of 32-37 (Fig. 4a). The un-cluster sample (hadal sediment of 0-1 cm at A4 station) was characterized by relatively longer alkyl chains (up to 42 C atoms) than Cluster 1 (Fig. 4a).

Overall, the degree of unsaturation (i.e., number of double bounds) within clusters was variable (Fig. 4b). Cluster 1 predominantly consisted of fully saturated and mono-unsaturated IPLs, except for PG that showed 2 double bonds in average. In Cluster 2, the fatty acids of DGCCs were distinctly variable, although they exhibited 2 unsaturations on average. A similar pattern was observed in DGDGs with an average of 2.5 unsaturations (Fig. 4b). DGTS, MGDGD, PC and SQDG showed zero to 1 unsaturation, whereas DGTA, PE and PG exhibited between 1 and 2.5 unsaturations. Cluster 3 showed more than 5 unsaturations on average for DGCC, unlike other IPL classes that did not exceed 2 unsaturations. In Cluster 4, PG and DGCC presented ~ 3 and ~ 5 unsaturations on average. Also, on average, DGDG and SQDG exhibited 2 unsaturations, MGDG and Others were mono-unsaturated, and DGTS were saturated (Fig. 4b). Additionally, the ratio of total unsaturated fatty acids to total saturated fatty acids in IPLs increased from (on average) ~ 0.9 in all water column samples (2-76 Bars) to ~ 2.7 in the bathyal (54-113 Bars) and hadal sediments (777-810 Bars) (Fig. 5).

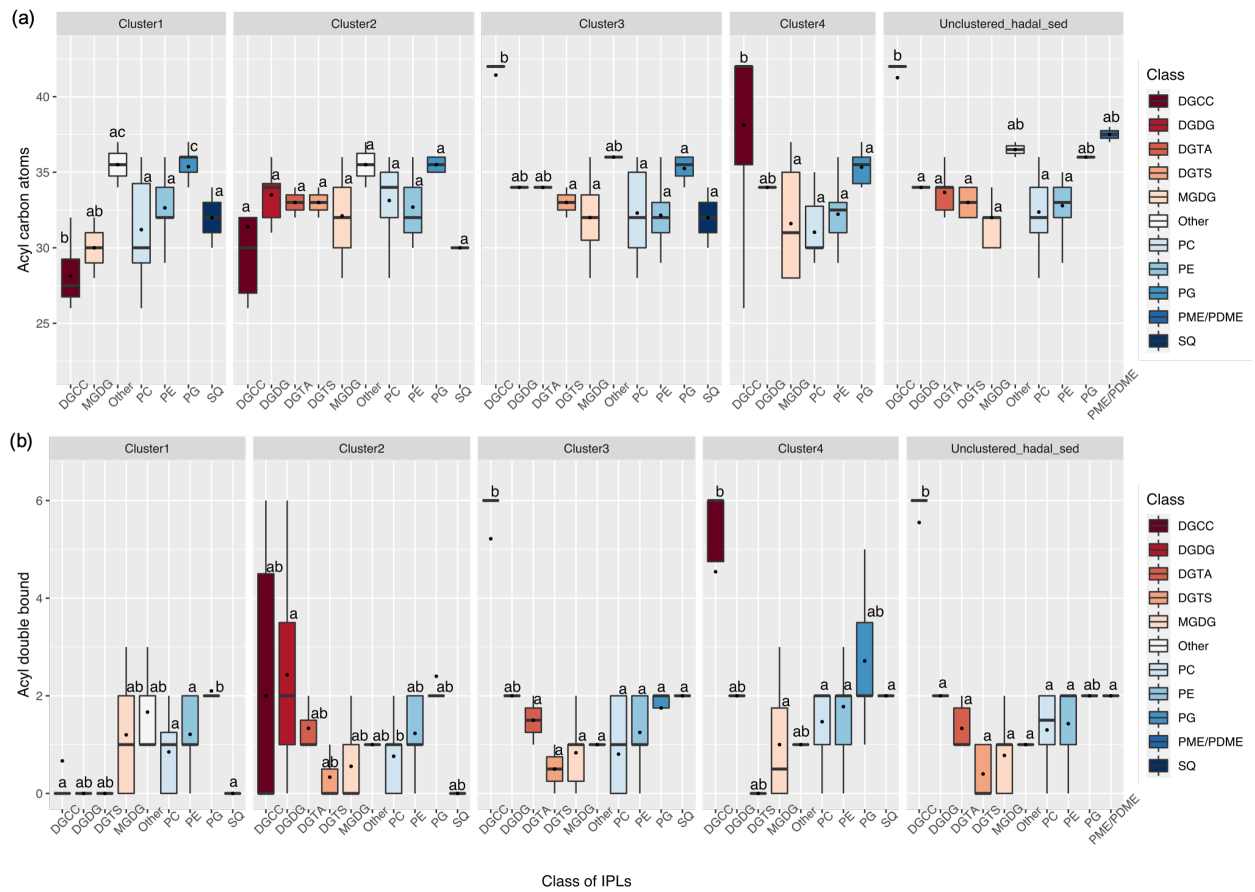


Figure 4. Total number of acyl carbon atoms (a) and acyl double bonds (b) in IPL classes across the distinct clusters shown in Fig. 2. The letters “a” and “b” indicate the presence of statistically distinct groups ($p < 0.05$) from both ANOVA and post-hoc Tukey HSD tests, respectively.

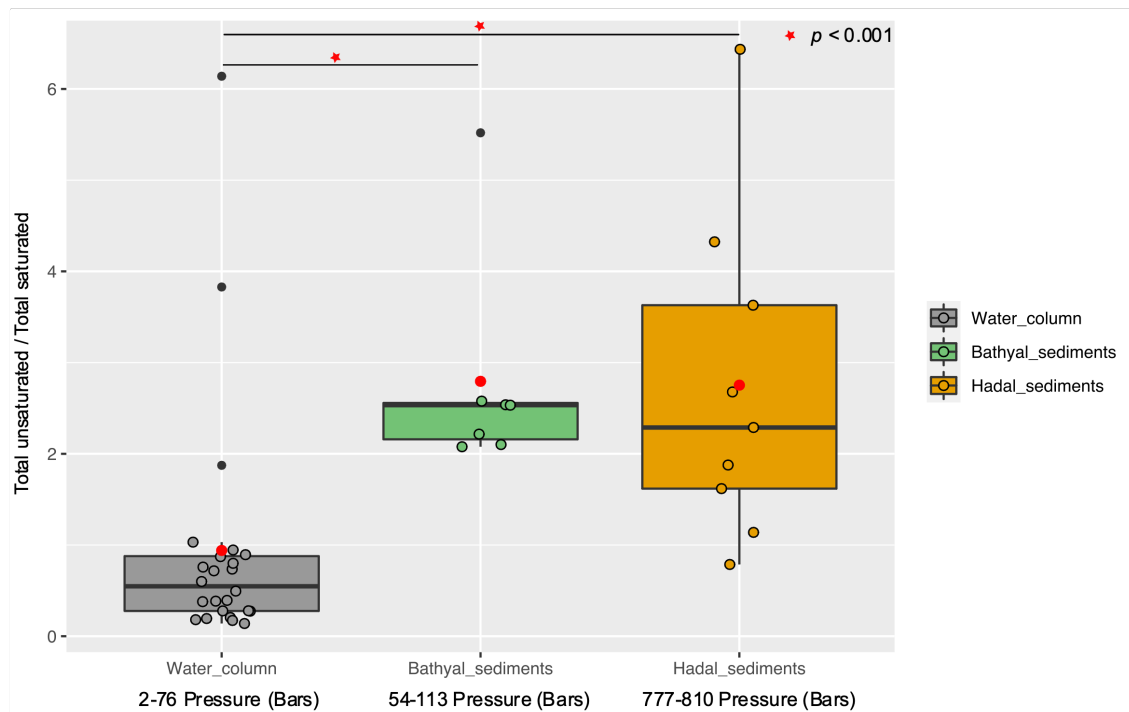


Figure 5. Boxplot showing the ratio of total unsaturated fatty acids to total saturated fatty acids derived from IPLs present in water column samples (Cantarero et al., 2020) and sediments of the Atacama Trench (this study). Red circles indicate the average value in each environment. Wilcoxon test (p -value < 0.001) indicates that sediments have statistical ratios higher than the water column (horizontal lines and red stars).

3.4 Unique IPLs in hadal sediments of the Atacama Trench

Water-column particles and bathyal-hadal sediments shared 242 (96.1%) IPL structures (Fig. 6a), while hadal sediments and water-column particles shared 14 (0.02%), and hadal and bathyal sediments shared 55 (3.6%). Of all the analyzed IPLs reported in this study, eight of them were unique to the Atacama Trench sediments and are not present in shallower sediments nor the overlying water column. They include five glycolipids (SQDG-42:11, SQDG-23:0, DGDG-35:1, DGDG-35:2 and DGDG-37:1), two phosphatidyl-inositols (PI-diOH-Ext-AR and PI-OH-AR), and one ornithine lipid (OL-37:6). While unique to hadal sediments, their total concentration was low ($\sim 53.32 \text{ ng g}^{-1}$ sediment) and they contributed $\sim 0.00012\%$ of the total IPL pool (Fig. 6a). We then performed a cluster analysis to compare IPLs in deep-sea surface sediments against IPLs reported in the overlying water column (Cantarero et al., 2020; Fig. 6b). Cluster 1 comprised samples from the core OMZ in the free-living fraction (AU p -value of 100%). Cluster 2 comprised samples from both the upper and lower oxyclines (~ 14 -60 m) as well as from the chlorophyll maximum (AU p -value of 99%). Cluster 3 comprised bathyal and hadal samples (AU p -value of 99%). Cluster 4 mostly comprised the deepest water column sample (mesopelagic region at 750 m) and hadal samples (AU p -value of 98%; Fig. 6b). We also compared IPLs in hadal and bathyal sediments against the pool of IPLs reported as diagnostic of the planktonic community inhabiting the chlorophyll maximum in the upper water column (Cantarero et al., 2020), and thus assess their export and stability through their transit to the deep-sea. Notably, these IPLs from this region of the water column only represent ~ 0.001 - 0.005% and 0.002 - 0.03% of the total IPL pool in hadal and bathyal sediments, respectively (Fig. S3).

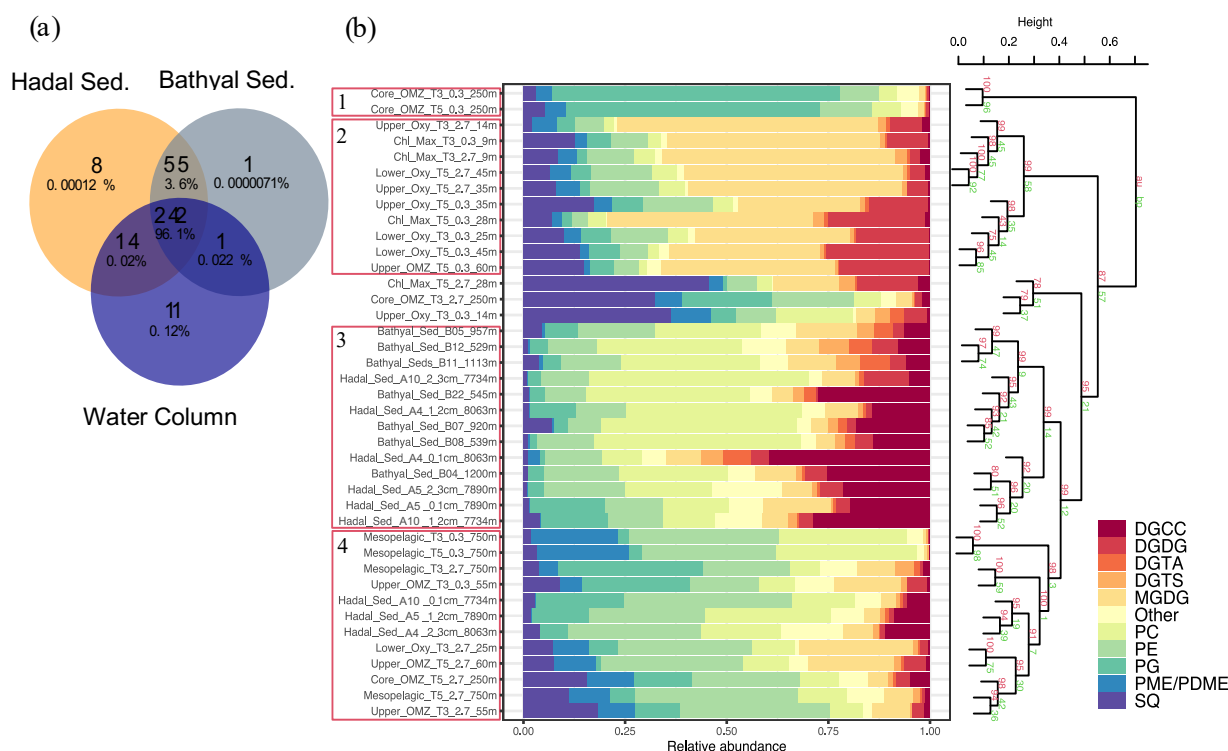


Figure 6. Comparison of IPLs in bathyal and hadal sediments (this study) and the overlying water column (Cantarero et al., 2020). (a) Venn diagram showing the number and percentage of unique and shared IPL molecules between these three environments. (b) Cumulative bar charts of IPL fractional abundances in each sample. Samples were grouped according to arithmetic mean (UPGMA) hierarchical clustering based on Euclidean distances. The cluster analysis on the right-hand side shows approximately unbiased (AU) and bootstrap probability (BP) in red and green numbers, respectively, whereas p-values are shown at branching points. Clusters with AU ≥ 95% confidence are highlighted in red on the left-hand side.

We found a high degree of heterogeneity in total IPL concentrations among sites and different sediment levels (0–1, 1–2, 2–3 cm) in the Atacama Trench, which were an order of magnitude higher than bathyal sediments (see Figs. S4a, S4b). Hadal sediments at station A10 (7,734 m) showed a large range of phospholipid concentrations (~47–2,698 ng g⁻¹ sediment) (Fig. S4b). Although the highest total IPL abundances were observed at hadal station A10 (Fig. S4b), the greatest diversity in IPL composition was observed in the 0–1 cm of the hadal station A4, previously referred to as un-clustered (see Fig. 2). The most abundant IPL class in hadal sediments were phospholipids, PCs (~41–2,698 ng g⁻¹ sed.), PEs (~26–1,813 ng g⁻¹ sed.) and PGs (5–937 ng g⁻¹ sed.). The concentration of IPLs normalized by TOC (ng IPL/g TOC) showed maximum values in the hadal station A10 (~497 µg IPL/g TOC), followed by lower values in the hadal stations A5 and A4 of ~291 and ~75 µg IPL/g TOC, respectively (Fig. S5).

4. Discussion

4.1 Potential sources of phospholipids

PG (Phosphatidylglycerol)

Phospholipids are common constituents of cellular membranes in most microorganisms (Ratledge and Wilkinson, 1988). Since PGs play an essential role in photosynthesis (Wada and Murata, 2007), they have therefore been mainly identified in algal and bacterial photoautotrophs (Dowhan, 1997; Sato et al., 2000; Gombos et al., 2002). However, their biological origin is highly diverse, and also includes heterotrophic bacteria (Oliver and Colwell, 1973; Van Mooy et al., 2009; Pendorf et al., 2011b; Carini et al., 2015; Sebastián et al., 2016), methylotrophs (Batrakov and Nikitin, 1996), methanotrophic bacteria (Makula, 1978), *Pelagibacter ubique* (Van Mooy et al., 2009), and barophilic bacteria (e.g., DB21MT-2 and DB21MT-5) isolated from sediments from the Marianas Trench (Fang et al., 2000).

The hierarchical cluster analysis on variations in the relative abundance of PGs suggests that several compounds maintained a similar proportion in bathyal and hadal sediments, which differs from the water column (Fig. S6). Most PGs in the bathyal and hadal sediments have long acyl carbon chains (C₃₄-C₄₁), and they show odd- and even-numbered polyunsaturated fatty acids (Fig. S6). The average chain-lengths of even-numbered *n*-C₁₈, *n*-C₂₀ and *n*-C₂₂ fatty acids, mostly in PCs and PGs, are indicative of algal inputs (Kaneda, 1991; Thompson Jr, 1996; Bergé and Barnathan, 2005; Brandsma et al., 2012). However, since these PGs were not dominant in the water column, a source from deeper environments is likely. Specifically, PG-DAG-36:2, PG-DAG-35:2, PG-DAG-36:5, PG-DAG-37:2, and PG-DAG-41:4 are the dominant constituents of this IPL class in hadal-bathyal sediments (Fig. 7; Fig. S6). PG-DAG-36:2 has been described in surface waters of the North Sea and also detected in picoeukaryotes (Brandsma et al., 2012), and in heterotrophic bacteria in surface waters of the open South Pacific Ocean (Van Mooy and Fredricks, 2010). However, these PGs are not dominant in the water column near the Atacama Trench (Cantarero et al., 2020). On the other hand, PG-DAG-35:2, PG-DAG-36:5, PG-DAG-37:2 and PG-DAG-41:4 are not commonly reported in water-column studies. Thus, it is possible that PGs present in the Atacama Trench sediments derive from *in situ* microbial production, although downslope and lateral transport of labile OM cannot be ruled out. PG-DAG-36:2 (Fig. 3) is the PG contributing most to the dissimilarity within the cluster containing only hadal sediments (Cluster 1 in Figure 2). Thus, this lipid appears to be more representative of *in situ* microbial production in this environment.

PE (Phosphatidylethanolamine)

PE and its methylated derivatives (PME, PDME) have been predominantly reported in membranes of diverse bacterial sources, including heterotrophic bacteria (Van Mooy and Fredricks, 2010; Schubotz et al., 2018a), nitrifying/denitrifying bacteria (Goldfine and Hagen, 1968), sulfate-reducing bacteria (Rütters et al., 2001; Sturt et al., 2004), sulfur-oxidizing bacteria (Barridge and Shively, 1968; Imhoff, 1995; Wakeham et al., 2012), methanotrophic bacteria (Makula, 1978; Sturt et al., 2004), and barophilic bacteria (Fang et al., 2000).

PEs showed a similar distribution in bathyal and hadal sediments (Fig. S7), where they are dominated by long-chain (C₃₆₋₄₄) polyunsaturated fatty acids, contrary to the shorter chains (C₂₈₋₃₆) of saturated and monounsaturated fatty acids present in the water column. PE-DAG-32:1, PE-DAG-32:2, and PE-DAG-33:1 are the dominant PE compounds of bathyal and hadal sediments (Fig. 7). These IPLs have been previously reported in heterotrophic bacteria (Van Mooy and Fredricks, 2010; Brandsma et al., 2012). On the other hand, fatty acids in PEs including monounsaturated and polyunsaturated (e.g., C_{20:5} and C_{22:6}) have been reported in barophilic bacteria isolated from

sediments from the Marianas Trench (Fang et al., 2000). Thus, although we cannot confidentially rule out other sources, it is possible that PEs present in the AT sediments predominantly derive from *in situ* production by barophilic heterotrophic bacteria. PE-DAG-32:1, PE-DAG-32:2 and PE-DAG-33:1 (Fig. 3) are the PEs that contributed most to the dissimilarity within the cluster containing only hadal sediment samples (Cluster 1 in Figure 2). Thus, this cluster appears to be representative of *in situ* microbial production in this environment.

PC (Phosphatidylcholine)

PCs were amongst the most diverse (43 structures: Fig. S8) and abundant phospholipid class in hadal sediments (Fig. S4). PC is the major membrane-forming phospholipid in eukaryotes (Lechevalier, 1988; Sohlenkamp et al., 2003; Van Mooy et al., 2006; Van Mooy and Fredricks, 2010). Additionally, PC has been reported to be a major DAG in zooplankton, from protozoa to copepods and krill (Patton et al., 1972; Mayzaud et al., 1999; Lund and Chu, 2002). However, genomic data indicates that more than 10% of all bacteria possess the genetic machinery for PC biosynthesis (Sohlenkamp et al., 2003). PC has also been reported in nitrifying bacteria (Lam et al., 2007), photoheterotrophic bacteria (Koblížek et al., 2006; Van Mooy et al., 2006), and barophilic bacteria (Fang et al., 2000). In surface sediments of the Black Sea (2000 m), PCs were related to algal material rapidly exported from surface waters (Schubotz et al., 2009a).

Hadal and bathyal sediments, in addition to two OMZ core stations, were clustered in the PC class (AU p-value of 97%; Fig. S8). This cluster showed PCs with long (C₃₃₋₃₈) and polyunsaturated fatty acids (up to 10 unsaturations). The dominant constituents were PC-DAG-35:0, PC-DAG-30:2, PC-DAG-30:1, PC-DAG-33:2, PC-DAG-35:1, PC-DAG-29:2, PC-DAG-32:1, and PC-DAG-36:2 (Fig. 7; Fig. S8). PC-DAG-36:2 and PC-DAG-30:1 have been associated with phytoplankton detritus (Schubotz et al., 2009a) and bacteria (Brandsma et al., 2012), whereas PC-DAG-32:1 has been associated with picoeukaryotes (Brandsma et al., 2012).

Since the most abundant PCs in Cluster 1 have not been reported as dominant structures in any specific environment before, they are possibly produced *in situ*, although downslope and/or lateral transport cannot be ruled out. Among bacteria, those membranes reported to contain PC belong to the alpha and gamma subgroups of the proteobacteria (Sohlenkamp et al., 2003). Given that these bacterial groups are abundant in trench samples from Puerto Rico (Eloe et al., 2011), the Mariana (Nunoura et al., 2015) and recently in the Atacama Trench (Schauberger et al., 2021), it is possible that PCs present in high abundance in the Atacama Trench are consistent with high abundance of proteobacteria in these regions. Given their general known association and abundance in Atacama Trench sediments (Fig. S4), they likely derive primarily from bacterial, but also possibly from fungi or metazoan sources that have not yet been studied, and to a lesser extent from phytoplankton. Indeed, fungal strains isolated from the water column and sediment in the ESTP off Chile reported high levels of polyunsaturated fatty acids and PCs (Gutiérrez et al., 2020), whereas a high fungal diversity associated with denitrification potential was reported in the Yap Trench (Gao et al., 2020). The latter suggests that eukaryotic PCs in hadal sediments could be much more diverse in origin than previously thought.

PME/PDME (Phosphatidyl(di)methylethanolamine)

PME/PDMEs have been observed in association with methanotrophic bacteria (Makula, 1978; Goldfine, 1984; Fang et al., 2000), sulfide oxidizer bacteria (Barridge and Shively, 1968), sulfate-reducing bacteria, mainly *Desulfobulbus spp* (Rossel et al., 2011), Proteobacteria (Oliver and Colwell, 1973; Goldfine, 1984), and barophilic bacteria from the Mariana Trench (Fang et al., 2000). Additionally, the occurrence of PME-DEG at some hadal stations suggests the presence of sulfate-reducing bacteria (Rütters et al., 2001; Sturt et al., 2004). PME/PDMEs exhibited their lowest abundance ($\sim 10 \text{ ng g sed}^{-1}$) in sediment samples compared to other phospholipids (Fig. S4b). In the bathyal and hadal sediments they were clustered (AU p-value of 97%) and dominated by PDME-DAG-33:1, PME-DAG-37:2, PME-DAG-34:2, PME-DAG-31:1, and PME-DEG-33:0 (Fig. S9a). PME-DEG-33:0 has been shown to correlate with high NO_2^- in the overlying water column of this area (Cantarero et al., 2020), which could suggest a potential association with denitrification processes. These structures have also been reported in the deep chemocline of the Cariaco basin (Wakeham et al., 2012), suggesting a potential chemoautotrophic and/or heterotrophic source. The distribution of these compounds is different from the water column, which is dominated by the saturated PME-32:0, PME-DAG-30:0, and PME-DAG-31:0 (Fig. S9a and S16; Cantarero et al., 2020). Thus, and similar to other lipid classes, they most likely derive from *in situ* production in hadal sediments rather than from the water column, although other sources such as downslope and/or lateral transport cannot be ruled out. No particular PME/PDME were found to contribute to the dissimilarity between the cluster containing only hadal sediment samples (Cluster 1 in Figure 2) and other sediment samples.

4.2 Potential sources of glycolipids

MGDG (Monoglycosyldiacylglycerol)

Due to their dominant occurrence in chloroplast thylakoid membranes (Murata and Siegenthaler, 1998) and particularly in cyanobacteria (Heinz, 1977; Harwood, 1998; Wada and Murata, 2007; Van Mooy and Fredricks, 2010), but also in heterotrophic bacteria (Popendorf et al., 2011b), MGDGs are probably the most abundant IPLs on earth (Gounaris and Barber, 1983).

The hierarchical cluster groups MGDGs in bathyal (AU p-value of 90%) and hadal (AU p-value of 98%) sediments (Fig. S10). The most abundant MGDGs in the bathyal and hadal sediments were MGDG-28:0, MGDG-32:1, MGDG-30:1, MGDG-32:0 and MGDG-37:3. MGDG-28:0, and MGDG-30:1, which are ubiquitous along the oxycline of the overlying OMZ (Fig. 7; Cantarero et al., 2020), in addition to MGDG-32:1. MGDG-32:0 has been reported in waters of the eastern south Pacific (Van Mooy and Fredricks, 2010). Thus, the occurrence of these MGDGs in sediment could indicate at least some export of labile OM from surface waters. On the other hand, MGDG-37:3 does not appear to be a dominant structure in any specific environment in the literature, which suggests a likely *in situ* production.

DGDG (Diglycosyldiacylglycerol)

DGDGs are commonly found in membranes of eukaryotic algae and cyanobacteria (Wada and Murata, 1998; Sakurai et al., 2006; Kalisch et al., 2016). DGDGs clustered together in bathyal and hadal sediments (AU p value of 96%) whereas their distribution differed from the water column (Fig. S11). The most abundant DGDGs in hadal and bathyal sediments of the Atacama Trench was DGDG-34:2 (Fig 7), which has been previously reported in

cyanobacterial strains isolated (da Costa et al., 2020), but has not been previously reported as abundant in the water column. In contrast, DGDG-30:0, which is widely distributed in the water column of this region (Cantarero et al., 2020), is consistently present in hadal and bathyal sediment samples although at very low abundances (Fig. 7). Thus, although DGDGs account for less than ~5% of the total IPL pool (Fig. 6b), except for station A10 (2-3 cm) where they reach ~10%, their presence in bathyal and hadal sediments is indicative of at least some export of labile OM from surface waters.

SQDG (Sulfoquinovosyldiacylglycerol)

SQDG are predominantly produced by photoautotrophs (Van Mooy et al., 2006; Popenorf et al., 2011b), including various groups of diatoms, brown and green algal chloroplast membranes (Harwood, 1998), and cyanobacteria (Siegenthaler, 1998; Wada and Murata, 1998). SQDGs have also been found in bacteria from the α - and γ -proteobacterial lineages (Benning, 1998). In the overlying water column of the Atacama Trench, Cantarero et al., (2020) suggested a higher contribution of SQDGs from cyanobacteria than algae. Also, SQDGs found in the deep Atlantic (down to ~4,000-5,000 m) appear to indicate a source and export from surface waters (Gašparović et al., 2018).

SQDGs showed a consistent distribution in bathyal and hadal sediments, where they are dominated by long-chain (C_{36-44}) fatty acids (Fig. S12). This is contrasting to their distribution in the overlying water column where they are dominated by shorter chain (C_{28-36}) saturated fatty acids (Cantarero et al., 2020). SQDG-30:0, SQDG-32:0, SQDG-30:2, and SQDG-38:4 were the dominant SQDG constituents of bathyal and hadal sediments (Fig. 7). SQDG-30:0 and SQDG-30:2 have been reported in bacteria in North Sea surface waters (Brandsma et al., 2012), in cyanobacteria of the eastern subtropical South Pacific (Van Mooy and Fredricks, 2010), and in plankton detritus from surface sediments of the Black Sea (Schubotz et al., 2009a). Furthermore, SQDG-30:0 is abundant in surface waters of our study area and SQDG-38:4 has been correlated with NO_3^- (Cantarero et al., 2020). The observed differences in the distribution of SQDGs in deep sediments compared to the water column suggests an *in situ* production of previously poorly characterized compounds, in addition to at least some export from surface waters.

4.3 Potential biological sources of betaine lipids

DGTS (Diacylglyceryl trimethylhomoserine)

DGTSs have diverse biological origins, being found in a wide range of eukaryotes (Sato, 1992; Dembitsky, 1996; Kato et al., 1997; Van Mooy et al., 2009), photoheterotrophic bacteria (Benning et al., 1995; Geiger et al., 1999), photoautotrophic bacteria (Popenorf et al., 2011b) including cyanobacteria (Řezanka et al., 2003), and members of the α -Proteobacteria subdivision (López-Lara et al., 2003). Schubotz et al. (2018) showed DGTS with varying fatty-acid compositions in the OMZ system of the eastern tropical North Pacific, especially in OMZ waters, indicating that these compounds can be biosynthesized by a wider range of source organisms than previously thought.

Consistent with other IPL classes, DGTSs of the bathyal and hadal samples were grouped in the same cluster (AU p-value of 98%) and differed from the water column (Fig. S13). However, several DGTSs are shared between

surface waters (9-60 m) and deep sediments. Indeed, the most abundant DGTSs in bathyal and hadal sediments (DGTS-34:0, DGTS-32:1, DGTS-26:0, DGTS-34:1, DGTS-32:0, and DGTS-25:0; Fig. 7; Fig. S13) are also prominent in the chlorophyll maximum in the eastern subtropical South Pacific (Van Mooy and Fredricks, 2010, and Cantarero et al., 2020). Therefore, their presence in hadal sediments suggest the export of some labile OM from the euphotic zone, although we cannot rule out other sources.

DGTA (Diacylglyceryl hydroxymethyl-trimethyl- β -alanine)

DGTAs have been widely reported in eukaryotic phytoplankton (Araki et al., 1991; Dembitsky, 1996; Cañavate et al., 2017), mainly in diatoms (Volkman et al., 1989; Zhukova, 2005; Gómez-Consarnau et al., 2007), and are also especially abundant in cultures of Prymnesiophytes and Cryptophytes (Kato et al., 1997). DGTAs have also been found in cyanobacteria (Brandsma et al., 2012) and heterotrophic bacteria (Popendorf et al., 2011a; Sebastián et al., 2016).

DGTAs in bathyal and hadal sediments are mainly composed of longer (C₂₈-C₄₂) and polyunsaturated (1-12) fatty acids compared to those present in the shallowest region of the overlying water column, composed of shorter and saturated fatty acids (Fig. S14). In the overlying water column, these compounds are associated with relatively high chlorophyll and O₂ concentrations (Cantarero et al., 2020), similar to North Sea surface waters (Brandsma et al., 2012). To the best of our knowledge, the dominant DGTAs in hadal and bathyal sediments (Fig. 7; Fig. S14) have not been previously reported as dominant IPLs in other environments. Whereas no specific biological sources in hadal sediments are known, the structures containing between 30 and 38 carbon atoms might be characteristic of this type of environment.

DGCC (Diacylglycerylcarboxy-N-hydroxymethyl-choline)

Our knowledge of DGCC sources is limited. They have been found in membranes of Prymnesiophyte algae (Kato et al., 1994), mainly in *Pavlova lutheria* (Kato et al., 1994; Eichenberger and Gribi, 1997), and in *E. huxleyi* (Volkman et al., 1989; Pond and Harris, 1996; Van Mooy and Fredricks, 2010). Additionally, they have also been reported in the diatom *Thalassiosira pseudonana* (Van Mooy et al., 2009).

The most abundant IPL from the entire data set of Bathyal and hadal sediments is DGCC-42:6 (Fig. 7; Fig. S15). This is the compound with the largest number of C atoms (42) and unsaturation (6) in all IPLs detected in this study. DGCCs with long-chain, polyunsaturated fatty acids (i.e., C_{38:6}, C_{40:10}, C_{42:11}, C_{44:12}) have been previously reported in phytoplankton (Hunter, 2015; Van Mooy and Fredricks, 2010). However, the most abundant DGCCs in hadal sediments have, to the best of our knowledge, not been previously reported, which highlights their potential as biomarkers of deep-sea sediments. However, 3 hadal stations clustered in a separate group (see Fig. S15), were dominated by DGCC-27:0, and did not contain DGCC-42:6, indicating that this IPL probably derives from allochthonous sources.

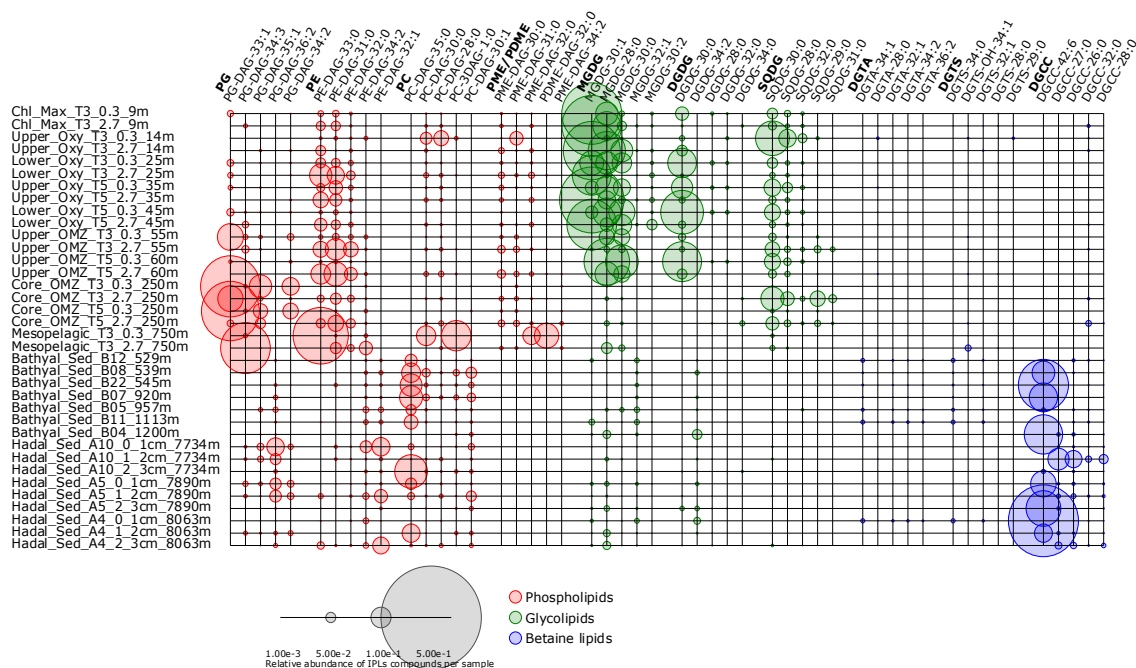


Figure 7. Relative abundance of the five most abundant individual IPLs contributing to each IPL class. Circle size is proportional to the relative abundance of IPL compounds per sample. Samples are organized along the Y axis by depth, whereas phospholipids, glycolipids, and betaine lipids are shown in colors. The legend provides a scale for circumference size.

4.4 Potential biological sources of other lipids

Glycosidic ceramides (Gly-Cer) have been reported in eukaryotic algae such as Prymnesiophyte (Vardi et al., 2009), and have also been shown to be abundant in water columns of OMZ systems (Schubotz et al., 2009b, 2018; Cantarero et al., 2020). In general, the overlying water column shows Gly-Cer with ceramide chain, and polyunsaturated fatty acids with C₂₁₋₃₈. However, these structures are scarce in the bathyal and hadal sediments (see Fig. S9b), which could reflect a deficient export from surface waters due to intense remineralization. On the other hand, Ornithine lipids (OL), phosphatidylinositol (PI), PC-AEGs and other unidentified phospholipids were also present in deep sediments (Fig. S9b). Some PIs and OLs have been reported in sulfate-reducing bacteria (Sturt et al., 2004; Bühring et al., 2014), whereas PC-AEGs have been reported in bacteria inhabiting water columns with reduced oxygen concentration (Schubotz et al., 2018b). Thus, the high relative abundance of PC-AEG-34:3 in hadal and bathyal sediments (Figs. S9b and S16) could be indicative of anaerobic microbial processes. PC-AEG-34:3 contributed the most to the dissimilarity between the cluster containing only hadal sediment samples (Cluster 1 in Figs. 2, and 3), thus suggesting an *in situ* microbial production, although we cannot confidentially rule out other sources.

4.5 Allochthonous versus autochthonous IPLs in the Atacama Trench

Given their rapid degradation after cell death (White et al., 1979; Harvey et al., 1986; Logemann et al., 2011), IPLs are typically considered markers of living or recently dead cells (White et al., 1979; Harvey et al., 1986; Petersen et al., 1991; Lipp et al., 2008). The distribution of IPLs in bathyal and hadal sediments exhibits a high degree of similitude, as demonstrated by the hierarchical analysis (Cluster 1 in Fig. 8a), the NMDS (Fig. 8b), and the SIMPER analysis (Cluster 1 in Table S1). The deep-sea surface sediments showed weak clustering with the

IPLs reported in the overlying water column by Cantarero et al. (2020) (Fig 9a). Additionally, water column samples exhibit a larger degree of separation than sediments (ANOSIM, $R = 0.78$; $P < 0.01$; Fig. 8b) and are broadly clustered by geochemical environments (Cantarero et al., 2020). The low abundance of IPLs characteristic of organisms inhabiting the chlorophyll maximum in deep-sea sediments of the Atacama Trench ($<0.005\%$ of the total IPL pool; Fig. S3) suggests minimal export of labile organic compounds from the upper ocean. This result implies rapid IPL degradation during sinking in the water column, which is consistent with experimental degradation rates (Westrich and Berner, 1984; Logemann et al., 2011) and first-order POM sinking rates. Indeed, by using the experimentally calculated kinetic degradation rate constants (k') of ester-bound IPLs by Logemann et al. (2011), and the sinking rate of particles from surface waters to 4000 m (20–100 m/day; Billett et al., 1983; Danovaro et al., 2014), we calculated that $\sim 86\text{--}98\%$ ($k'_{t=80} = 0.033$ and $k'_{t=400} = 0.011$) of IPLs from surface waters should degrade by the time that particles reach depths of ~ 8000 m. These results are also in accord with studies indicating elevated benthic oxygen consumption rates resulting from intense microbial respiration of sinking OM reaching the sediment (Glud et al., 2013; Wenzhöfer et al., 2016). Thus, the pool of IPLs in hadal sediments appears to predominantly represent *in situ* microbial production, whereas the deep-sea microbial community in both bathyal and hadal sediments is similar despite their bathymetric zonation ($\sim 1,000\text{--}8,000$ m). Alternatively, we cannot rule out the possibility of new IPL production, particularly from heterotrophic and chemoautotrophic bacteria in micro niches of sinking particles reaching the deep-sea, and/or downslope and lateral sediment transport.

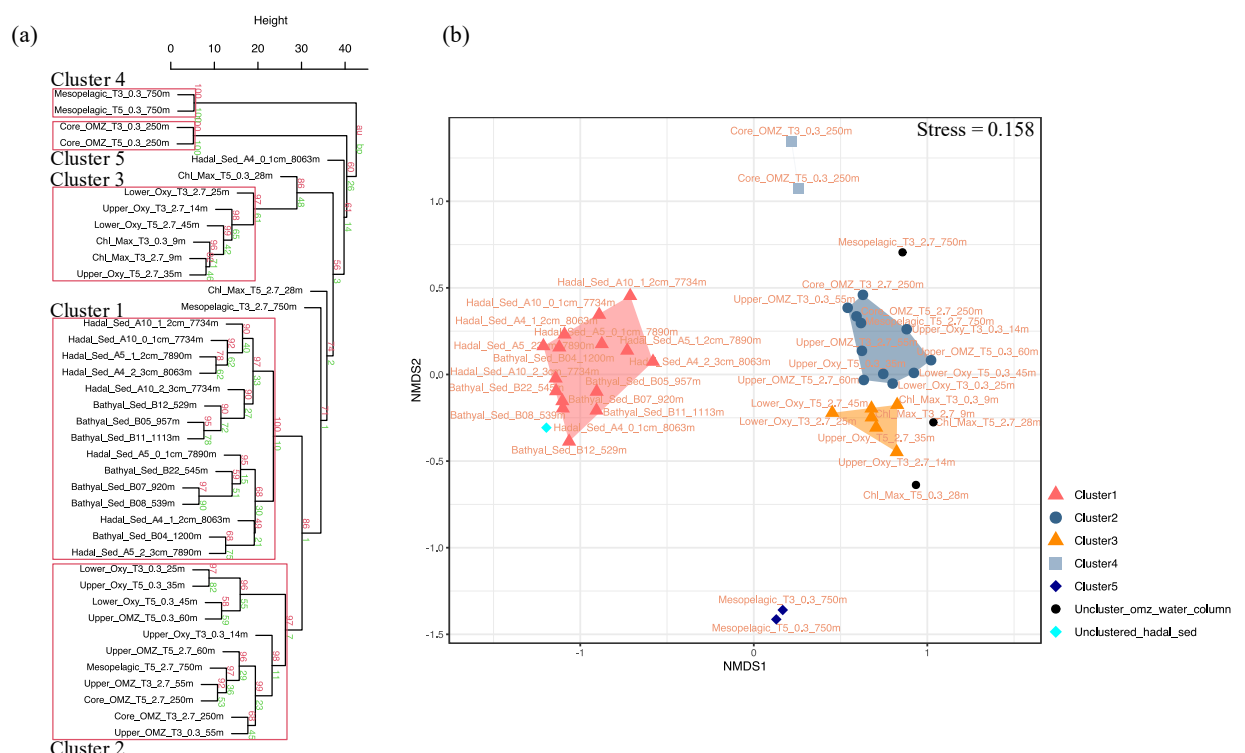


Figure 8. (a) Arithmetic mean (UPGMA) hierarchical clustering based on Euclidean distances calculated from IPLs in each sampling station. Red values are Approximately Unbiased (AU) p-values and green values are Bootstrap Probability (BP) for each node. Red boxes highlight clusters with 95% confidence. The number of bootstrap replicates is 10000. (b) Non-metric multidimensional scaling (NMDS) analysis of IPLs at each sampling station. The distance matrix was calculated based on the Bray–Curtis dissimilarity. The stress value of the final configuration was 15.8 %. Different symbols and colors represent the sample grouping from hierarchical clusters shown in panel a. Marine trenches receive organic carbon from a variety of sources and transport mechanisms. These include canyons and river systems that channel OM from land to coastal regions, aeolian transport, surface water

productivity, and *in situ* production, to name a few (Wenzhöfer et al., 2016; Tarn et al., 2016; Luo et al., 2017; Xu et al., 2018; Guan et al., 2019; Xu et al., 2021). Carbon flux events can increase the delivery of particulate carbon from surface waters to the seafloor (Poff et al., 2021), whereas river discharge and aeolian transport can result in enhanced terrestrial carbon (Xu et al., 2021). Mass wasting events are also known to create dynamic depositional conditions and strong spatial heterogeneity in OM distribution in marine trenches (Schauberger et al., 2021; Xu et al., 2021). While marine organic carbon appears to dominate sediments in the Japan (Schwestermann et al., 2021) Massau, and New Britain (Xu et al., 2020) trenches, the Atacama and Kermadec Trenches, on the other hand, have been reported to be dominated by terrigenous OM. Since our study only focuses on the most labile component of the total lipid pool, it predominantly traces labile and indigenous OM and not recalcitrant fractions of the lipid pool. The latter warrants further investigation.

In regions like the Japan trench, downslope sediment transport has been linked to earthquake-driven remobilization (Bao et al., 2018; Schwestermann et al., 2021). Whereas we lack sedimentological/geochemical data to discriminate if the top 3 cm of our hadal stations represent debris flows, turbidite, or mass wasting events, ongoing work in the Atacama Trench indicates heterogenic sediment deposition along the hadal zone (Matthias Zabel, pers. communication). Thus, the role of downslope transport as a mechanism to explain the high statistical similarity between bathyal and hadal sediments remains to be tested.

4.6 Characteristic IPLs of hadal and bathyal sediments

The IPLs that contribute most to the dissimilarity between the hierarchical cluster containing samples from the hadal and bathyal sediments (Cluster 1 of Fig. 8) and the water column (cluster 2, 3, 4 and 5 of Fig. 8) are represented in Fig. 9. The most characteristic IPLs of hadal and bathyal sediments are: DGCC-42:6, DGCC-27:0, DGCC-26:0, PC-DAG-35:0, PC-DAG-30:1, PC-DAG-30:2, PC-DAG-33:2, PC-DAG-32:1, PC-DAG-29:2, PE-DAG-32:1, PE-DAG-32:2, PE-DAG-33:1, PG-DAG-36:2, and DGDG-34:2, which we propose as potential markers for these environments. Even though DGCCs have been mainly related to algae membranes (Kato et al., 1994; Van Mooy et al., 2009), they are minor components of the water column in this area, suggesting the occurrence of an alternative source. In addition to DGCCs, the two other betaine lipids, DGTA and DGTS, exhibited five IPLs that were almost exclusively present in sediment samples (DGTA-34:1, DGTA-32:1, DGTA-34:2, DGTS-34:0 and DGTS-32:1, see Figure 11). We note that almost all the PC phospholipids in our study have not, to the best of our knowledge, been previously reported in the literature, which reinforces their use as markers of sedimentary *in situ* bathyal and hadal production.

The presence of a few MGDGs and SQDGs in hadal and bathyal sediments (~7% of the total IPL pool) indicates that at least some labile OM could derive from the shallow water column (see section 4.2). However, the most abundant IPLs in our sediment samples, DGCC-42:6, PC-DAG-35:0, PE-DAG-32:1 and PG-DAG-36:2 (19.8% of the total IPL pool; Fig. S16), are almost completely absent in the overlying water column (Fig. 9). This reinforces the idea that these IPLs most likely originate from *in situ* microbial production in sediments. The single most abundant IPL in sediments, DGCC-42:6, was not present in cluster 1, which only contains hadal sediments (Figs. 2 and 3). Instead, this compound is prominent in clusters 3, 4, and 5, containing both hadal and bathyal

samples. Thus, DGCC-42:6, as well as PC-DAG-35:0, which has the lowest relative abundance in the cluster with only hadal sediments, could be indicators of downslope transport from bathyal to hadal regions. We acknowledge that temporal variability in IPL production in the water column and sediment, as well as the lack of data on the largely uncharacterized hadal endemic microbial community, could complicate some of the phylogenetic and source associations of IPLs and warrant further investigation. Despite this, our study represents a step forward on the characterization of labile sources of OM sustaining hadal ecosystems.

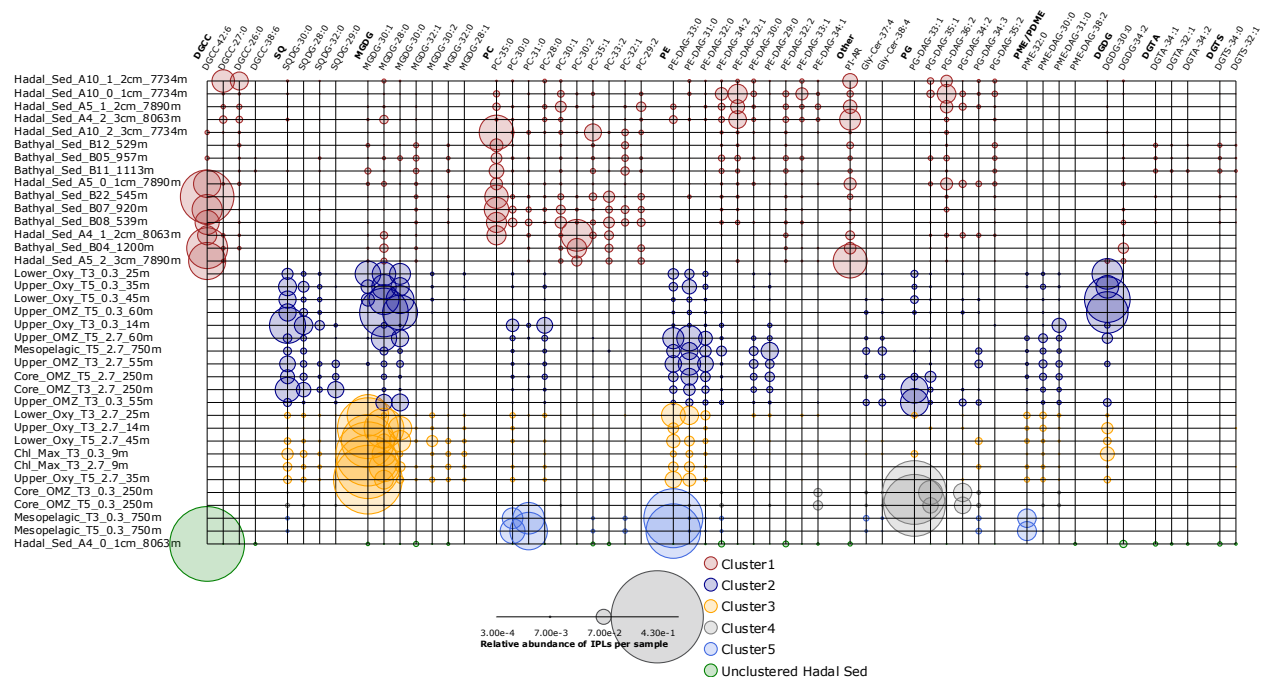


Figure 9. Relative abundance of individual IPLs that contribute most to the dissimilarity between clusters of Fig. 8 derived from the SIMPER analysis (Table S1). Circle size is proportional to the relative abundance of IPL compounds per sample. Samples are organized along the Y axis and shown in colors that match the hierarchical cluster analysis in Fig. 8. The legend shows the scale for circumference size.

4.7 Do IPLs reveal homeoviscous adaptation to the deep-sea environment?

Environmental factors such as pH, conductivity, temperature, and pressure impact the permeability and fluidity of cell membranes (Shaw, 1974; Macdonald, 1984; DeLong and Yayanos, 1985; Somero, 1992; Komatsu and Chong, 1998; Van Mooy et al., 2009; Carini et al., 2015; Sebastián et al., 2016; Siliakus et al., 2017; Boyer et al., 2020). Thus, organisms adapt to changes in environmental factors to maintain physiological homeostasis by altering their fatty acid composition (DeLong and Yayanos, 1985; Fang et al., 2000; Nichols et al., 2004; Siliakus et al., 2017). For instance, the combined physiological effects of high hydrostatic pressure and low temperature on prokaryotic membranes in laboratory cultures leads to the production of unsaturated lipids (DeLong and Yayanos 1985; Fang et al., 2000; Nichols et al., 2004; Zheng et al., 2020). However, few studies have been conducted using culture-independent techniques in search for potential adaptation mechanisms in organisms inhabiting the deep ocean (i.e., Zhong et al., 2020). We sought to understand whether the chemical composition of core fatty acids within different IPL classes (i.e., carbon length and unsaturation degree) reflects the combined

effects of the low temperature and high pressure typical of hadal settings. We show that PGs are abundant in hadal sediments of the Atacama Trench (Fig. S4). Bacterial strains isolated from Mariana Trench sediments contain PG as the most abundant class of phospholipids (Fang et al., 2000), which these authors presumed it could represent a physiological response to high pressure and low temperature. This has been confirmed by subsequent studies (Winter et al., 2009; Periasamy et al., 2009; Jebbar et al., 2015; Allemann et al., 2021). Cluster 1 in the boxplot analysis (Fig. 4) likely contains the most characteristic IPL classes of the hadal zone. In general, the phospholipids in this cluster exhibited fatty acid chains that are monounsaturated and saturated compared to other environments (Figs. 4a, b). Additionally, we observed an increase in the ratio of total unsaturated to saturated fatty acids in deep sediments compared to the water column (Fig. 5), which could reflect physiological adaptations of their biological producers. These results are in accord with studies indicating biosynthesis and incorporation of polyunsaturated fatty acids into phospholipid membranes of piezophilic bacteria (DeLong and Yayanos, 1985; Baird et al., 1985; Yano et al., 1998; Winter, 2002; Mangelsdorf et al., 2005; Winter and Jeworrek, 2009; Allemann et al., 2021). Thus, the chemical characteristics (C length and degree of unsaturation) of the most abundant IPLs in sediments of the Atacama Trench suggest homeoviscous adaptation to this type of environment by their source organisms, in addition to potentially indicating the occurrence of compounds that are unique to the endogenous community.

5. Conclusions

Bacterial and eukaryotic IPLs in surface hadal sediments from the deepest points of the Atacama Trench share characteristics with those in bathyal sediments and differ from those found in suspended particles from the upper 750 m of the water column, including the oxygen minimum zone. This indicates that: a) most IPLs abounding the upper water column are almost entirely degraded during their descent to the hadal seafloor, and b) IPLs found in hadal sediments are predominantly derived from in situ microbial communities.

The most dominant ester-bound IPL structures found in bathyal and hadal sediments show a great variety of phospholipids with varying degrees of unsaturation, most of them yet to be described, that are likely derived from yet poorly characterized bacterial and/or eukaryotes sources. Hadal sediments also exhibit unique glycolipid structures, such as SQDG-42:11, SQDG-23:0, DGDG-35:1, DGDG-35:2 and DGDG-37:1, that to the best of our knowledge, have not been reported in other environments. However, these lipids are present in low abundance and represent a small fraction (~0.00012%) of the total IPL pool. Furthermore, elevated ratios of unsaturated/saturated fatty acids in hadal sediments are likely indicative of homeoviscous adaptation to the high pressure and low temperatures characteristic of this extreme deep-sea environment.

An improved understanding of the phylogenetic, ecological, and metabolic association of IPLs present in the Atacama Trench could be achieved in future studies by the pairing of lipidomics with genomic techniques (e.g., microbial community composition, functional groups, lipid biosynthesis), in addition to a detailed sedimentological and biogeochemical characterization of sediments.

Author contribution

EF, OU, and JS designed the study. MZ contributed with the hadal samples from the HADES-ERC cruise. EF prepared, extracted, and analyzed samples from the HADES-ERC cruise with help from SC and ND under the supervision of JS. EF and SC processed results. EF, SC, and JS interpreted results. EF and PR-F performed statistical analyses. EF wrote the manuscript with contributions from SC, JS, and OU. All authors provided feedback on the manuscript. OU and JS funded the research.

Competing interests

The authors declare that they have no conflict of interest.

Acknowledgements

This work was supported by the Chilean Agency for Research and Development (grants ICN12_019-IMO and FONDECYT 1191360 to O. Ulloa). Additional support was provided by the Department of Geological Sciences and INSTAAR at the University of Colorado Boulder (to J. Sepúlveda), the European Research Council (Hades-ERC, grant agreement number 669947, to R.N. Glud), and the Max Planck Society. EF was also partially supported by the UCO 1866 Student Scholarship-2019, Directorate of Graduate Studies, Universidad of Concepción. We are thankful to the captains, crews, and scientists of the German RV *Sonne* cruises SO-261 (HADES-ERC) and SO-211 (ChiMeBo). In particular, we thank the chief scientists R.N. Glud and F. Wenzhöfer (HADES-ERC) and D. Hebbeln (ChiMeBo). The HADES-ERC and ChiMeBo cruises were funded by the European Research Council and the German Bundesministerium für Bildung & Forschung (BMBF), respectively. We also wish to thank Carina Lange and Silvio Pantoja for access to samples from the ChiMeBo cruise and M. Pizarro-Koch for the preparation of the three-dimensional map. We also thank L. Nuñez, B. Srain, R. Castro, A. Ávila, M. Mohtadi, R. De Pol-Holz, and G. Martínez-Méndez, for sample collection during the ChiMeBo cruise and/or laboratory assistance.

References

- Ahumada, R.: Producción y destino de la biomasa fitoplanctónica en un sistema de bahías en Chile central: una hipótesis, *Biol PesqChile*, 18, 53–66, 1989.
- Allemann, M. N. and Allen, E. E.: Genetic suppression of lethal mutations in fatty acid biosynthesis mediated by a secondary lipid synthase, *Appl. Environ. Microbiol.*, 87, 2021.
- Allen, E. E., Facciotti, D., and Bartlett, D. H.: Monounsaturated but not polyunsaturated fatty acids are required for growth of the deep-sea bacterium *Photobacterium profundum* SS9 at high pressure and low temperature, *Appl. Environ. Microbiol.*, 65, 1710–1720, 1999.
- Angel, M.: Detrital organic fluxes through pelagic ecosystems, in: *Flows of energy and materials in marine ecosystems*, Springer, 475–516, 1984.

- 815 Angel, M. V.: Ocean trench conservation, *Environmentalist*, 2, 1–17, 1982.
- 816 Araki, S., Eichenberger, W., Sakurai, T., and Sato, N.: Distribution of diacylglycerylhydroxymethyltrimethyl- β -
817 alanine (DGTA) and phosphatidylcholine in brown algae, *Plant Cell Physiol.*, 32, 623–628, 1991.
- 818 Baird, B.: Biomass and community structure of the abyssal microbiota determined from basin and Puerto Rico
819 trench sediments, *Benthic Ecol. Sediment. Process. Venezuela Basin-Past Present*, 61, 217–213, 1985.
- 820 Bao, R., Strasser, M., McNichol, A. P., Haghipour, N., McIntyre, C., Wefer, G., and Eglinton, T. I.: Tectonically-
821 triggered sediment and carbon export to the Hadal zone, *Nat. Commun.*, 9, 1–8, 2018.
- 822 Barridge, J. K. and Shively, J.: Phospholipids of the *Thiobacilli*, *J. Bacteriol.*, 95, 2182–2185, 1968.
- 823 Batrakov, S. G. and Nikitin, D. I.: Lipid composition of the phosphatidylcholine-producing bacterium
824 *Hyphomicrobium vulgare* NP-160, *Biochim. Biophys. Acta BBA-Lipids Lipid Metab.*, 1302, 129–137, 1996.
- 825 Benning, C., Huang, Z.-H., and Gage, D. A.: Accumulation of a novel glycolipid and a betaine lipid in cells of
826 *Rhodobacter sphaeroides* grown under phosphate limitation, *Arch. Biochem. Biophys.*, 317, 103–111, 1995.
- 827 Bergé, J.-P. and Barnathan, G.: Fatty acids from lipids of marine organisms: molecular biodiversity, roles as
828 biomarkers, biologically active compounds, and economical aspects, *Mar. Biotechnol.* 1, 49–125, 2005.
- 829 Biddle, J. F., Lipp, J. S., Lever, M. A., Lloyd, K. G., Sørensen, K. B., Anderson, R., Fredricks, H. F., Elvert, M.,
830 Kelly, T. J., Schrag, D. P., and others: Heterotrophic Archaea dominate sedimentary subsurface ecosystems off
831 Peru, *Proc. Natl. Acad. Sci.*, 103, 3846–3851, 2006.
- 832 Billett, D., Lampitt, R., Rice, A., and Mantoura, R.: Seasonal sedimentation of phytoplankton to the deep-sea
833 benthos, *Nature*, 302, 520–522, 1983.
- 834 Bligh, E. G. and Dyer, W. J.: A rapid method of total lipid extraction and purification, *Can. J. Biochem. Physiol.*,
835 37, 911–917, 1959.
- 836 Boyer, G. M., Schubotz, F., Summons, R. E., Woods, J., and Shock, E. L.: Carbon oxidation state in microbial
837 polar lipids suggests adaptation to hot spring temperature and redox gradients, *Front. Microbiol.*, 11, 229, 2020.
- 838 Brandsma, J., Hopmans, E., Philippart, C., Veldhuis, M., Schouten, S., and Damsté, J. S.: Temporal variations in
839 abundance and composition of intact polar lipids in North Sea coastal marine water, *Biogeosciences Discuss.*, 8,
840 8895, 2011.
- 841 Brandsma, J., Hopmans, E., Philippart, C., Veldhuis, M., Schouten, S., and Sinninghe Damsté, J.: Low temporal
842 variation in the intact polar lipid composition of North Sea coastal marine water reveals limited chemotaxonomic
843 value, *Biogeosciences*, 9, 1073–1084, 2012.

844 Bühring, S. I., Kamp, A., Wörmer, L., Ho, S., and Hinrichs, K.-U.: Functional structure of laminated microbial
845 sediments from a supratidal sandy beach of the German Wadden Sea (St. Peter-Ording), *J. Sea Res.*, 85, 463–473,
846 2014.

847 Cañavate, J. P., Armada, I., and Hachero-Cruzado, I.: Interspecific variability in phosphorus-induced lipid
848 remodelling among marine eukaryotic phytoplankton, *New Phytol.*, 213, 700–713, 2017.

849 Cantarero, S. I., Henríquez-Castillo, C., Dildar, N., Vargas, C. A., Von Dassow, P., Cornejo-D’Ottone, M., and
850 Sepúlveda, J.: Size-fractionated contribution of microbial biomass to suspended organic matter in the eastern
851 Tropical South Pacific oxygen minimum zone, *Front. Mar. Sci.*, 7, 745, 2020.

852 Carini, P., Van Mooy, B. A., Thrash, J. C., White, A., Zhao, Y., Campbell, E. O., Fredricks, H. F., and Giovannoni,
853 S. J.: SAR11 lipid renovation in response to phosphate starvation, *Proc. Natl. Acad. Sci.*, 112, 7767–7772, 2015.

854 Clarke, K. and Gorley, R.: Getting started with PRIMER v7, Primer-E Plymouth Plymouth Mar. Lab., 20, 2015.

855 da Costa, E., Amaro, H. M., Melo, T., Guedes, A. C., and Domingues, M. R.: Screening for polar lipids,
856 antioxidant, and anti-inflammatory activities of *Gloeotheca* sp. lipid extracts pursuing new phytochemicals from
857 cyanobacteria, *J. Appl. Phycol.*, 32, 3015–3030, 2020.

858 Danovaro, R., Della Croce, N., Dell’Anno, A., and Pusceddu, A.: A depocenter of organic matter at 7800 m depth
859 in the SE Pacific Ocean, *Deep Sea Res. Part Oceanogr. Res. Pap.*, 50, 1411–1420, 2003.

860 Danovaro, R., Snelgrove, P. V., and Tyler, P.: Challenging the paradigms of deep-sea ecology, *Trends Ecol. Evol.*,
861 29, 465–475, 2014.

862 DeLong, E. F. and Yayanos, A. A.: Adaptation of the membrane lipids of a deep-sea bacterium to changes in
863 hydrostatic pressure, *Science*, 228, 1101–1103, 1985.

864 Dembitsky, V. M.: Betaine ether-linked glycerolipids: chemistry and biology, *Prog. Lipid Res.*, 35, 1–51, 1996.

865 Dowhan, W.: Molecular basis for membrane phospholipid diversity: why are there so many lipids?, *Annu. Rev.*
866 *Biochem.*, 66, 199–232, 1997.

867 Eichenberger, W. and Gribo, C.: Lipids of *Pavlova lutheri*: cellular site and metabolic role of DGCC,
868 *Phytochemistry*, 45, 1561–1567, 1997.

869 Eloe, E. A., Shulse, C. N., Fadrosch, D. W., Williamson, S. J., Allen, E. E., and Bartlett, D. H.: Compositional
870 differences in particle-associated and free-living microbial assemblages from an extreme deep-ocean
871 environment, *Environ. Microbiol. Rep.*, 3, 449–458, 2011.

872 Fang, J., Barcelona, M. J., Nogi, Y., and Kato, C.: Biochemical implications and geochemical significance of
873 novel phospholipids of the extremely barophilic bacteria from the Marianas Trench at 11,000 m, *Deep Sea Res.*
874 *Part Oceanogr. Res. Pap.*, 47, 1173–1182, 2000.

875 Fernández-Urruzola, I., Ulloa, O., Glud, R., Pinkerton, M., Schneider W., Wenzhöfer, F. and Escribano, R:
876 Plankton respiration in the Atacama Trench region: Implications for particulate organic carbon flux into the hadal
877 realm, *Limnol. Oceanogr.*, 2021.

878 Fischer, J. P., Ferdelman, T. G., D'Hondt, S., Røy, H., and Wenzhöfer, F.: Oxygen penetration deep into the
879 sediment of the South Pacific gyre, *Biogeosciences*, 6, 1467–1478, 2009.

880 Gao, Y., Du, X. Xu, W., Fan, R., Zhang, X., Yang, S., Chen, X., Lv, J., Luo, Z. Fungal diversity in deep sea
881 sediments from east yao trench and their denitrification potential. *Geomicrobiol. J.*, 1–11, 2020.

882 Gašparović, B., Penezić, A., Frka, S., Kazazić, S., Lampitt, R. S., Holguin, F. O., Sudasinghe, N., and Schaub, T.:
883 Particulate sulfur-containing lipids: Production and cycling from the epipelagic to the abyssopelagic zone, *Deep*
884 *Sea Res. Part Oceanogr. Res. Pap.*, 134, 12–22, 2018.

885 Geiger, O., Röhrs, V., Weissenmayer, B., Finan, T. M., and Thomas-Oates, J. E.: The regulator gene *phoB*
886 mediates phosphate stress-controlled synthesis of the membrane lipid diacylglycerol-N, N, N-
887 trimethylhomoserine in *Rhizobium* (*Sinorhizobium*) *meliloti*, *Mol. Microbiol.*, 32, 63–73, 1999.

888 Glud, R. N., Wenzhöfer, F., Middelboe, M., Oguri, K., Turnewitsch, R., Canfield, D. E., and Kitazato, H.: High
889 rates of microbial carbon turnover in sediments in the deepest oceanic trench on Earth, *Nat. Geosci.*, 6, 284–288,
890 2013.

891 Glud, R. N., Berg, P., Thamdrup, B., Larsen, M., Stewart, H. A., Jamieson, A. J., Glud, A., Oguri, K., Sanei, H.,
892 Rowden, A. A., and others: Hadal trenches are dynamic hotspots for early diagenesis in the deep sea, *Commun.*
893 *Earth Environ.*, 2, 1–8, 2021.

894 Goldfine, H.: Bacterial membranes and lipid packing theory, *J. Lipid Res.*, 25, 1501–1507, 1984.

895 Goldfine, H. and Hagen, P.-O.: N-Methyl groups in bacterial lipids III. phospholipids of hyphomicrobia, *J.*
896 *Bacteriol.*, 95, 367–375, 1968.

897 Gombos, Z., Várkonyi, Z., Hagio, M., Iwaki, M., Kovács, L., Masamoto, K., Itoh, S., and Wada, H.:
898 Phosphatidylglycerol requirement for the function of electron acceptor plastoquinone QB in the photosystem II
899 reaction center, *Biochemistry*, 41, 3796–3802, 2002.

900 Gómez-Consarnau, L., González, J. M., Coll-Lladó, M., Gourdon, P., Pascher, T., Neutze, R., Pedrós-Alió, C.,
901 and Pinhassi, J.: Light stimulates growth of proteorhodopsin-containing marine Flavobacteria, *Nature*, 445, 210–
902 213, 2007.

903 Gooday, A. J., Bett, B. J., Escobar, E., Ingole, B., Levin, L. A., Neira, C., Raman, A. V., and Sellanes, J.: Habitat
904 heterogeneity and its influence on benthic biodiversity in oxygen minimum zones, *Mar. Ecol.*, 31, 125–147, 2010.

905 Gounaris, K. and Barber, J.: Monogalactosyldiacylglycerol: the most abundant polar lipid in nature, *Trends*
906 *Biochem. Sci.*, 8, 378–381, 1983.

907 Gutiérrez, M. H., Vera J., Srain B., Quiñones, R. A., Wörmer L., Hinrichs K.-U., and Pantoja, S. Biochemical
908 fingerprints of marine fungi: implications for trophic and biogeochemical studies. *Aquat. Microb. Ecol.*, 2020.

909 Guan, H., Chen, L., Luo, M., Liu, L., Mao, S., Ge, H., Zhang, M., Fang, J., and Chen, D.: Composition and origin
910 of lipid biomarkers in the surface sediments from the southern Challenger Deep, Mariana Trench, *Geosci. Front.*,
911 10, 351–360, 2019.

912 Grabowski, E., Letelier, R. M., Laws, E. A., and Karl, D. M.: Coupling carbon and energy fluxes in the North
913 Pacific Subtropical Gyre, *Nat. Commun.*, 10, 1895, 2019.

914 Hand, K., Bartlett, D., Fryer, P., Peoples, L., Williford, K., Hofmann, A., and Cameron, J.: Discovery of novel
915 structures at 10.7 km depth in the Mariana Trench may reveal chemolithoautotrophic microbial communities,
916 *Deep Sea Res. Part Oceanogr. Res. Pap.*, 160, 103238, 2020.

917 Harvey, H. R., Fallon, R. D., and Patton, J. S.: The effect of organic matter and oxygen on the degradation of
918 bacterial membrane lipids in marine sediments, *Geochim. Cosmochim. Acta*, 50, 795–804, 1986.

919 Harwood, J. L.: Membrane lipids in algae, in: *Lipids in photosynthesis: structure, function and genetics*, Springer,
920 53–64, 1998.

921 Hedges, J. I., Baldock, J. A., Gélina, Y., Lee, C., Peterson, M., and Wakeham, S. G.: Evidence for non-selective
922 preservation of organic matter in sinking marine particles, *Nature*, 409, 801–804, 2001.

923 Heinz, E.: Enzymatic reactions in galactolipid biosynthesis, in: *Lipids and lipid polymers in higher plants*,
924 Springer, 102–120, 1977.

925 Hiraoka, S., Hirai, M., Matsui, Y., Makabe, A., Minegishi, H., Tsuda, M., Rastelli, E., Danovaro, R., Corinaldesi,
926 C., Kitahashi, T., and others: Microbial community and geochemical analyses of trans-trench sediments for
927 understanding the roles of hadal environments, *ISME J.*, 14, 740–756, 2020.

928 Houston, J.: Variability of precipitation in the Atacama Desert: its causes and hydrological impact, *Int. J. Climatol.*
929 *J. R. Meteorol. Soc.*, 26, 2181–2198, 2006.

930 Hunter, J. E.: *Phytoplankton lipidomics: lipid dynamics in response to microalgal stressors*, PhD Thesis,
931 University of Southampton, 2015.

932 Ichino, M. C., Clark, M. R., Drazen, J. C., Jamieson, A., Jones, D. O., Martin, A. P., Rowden, A. A., Shank, T.
933 M., Yancey, P. H., and Ruhl, H. A.: The distribution of benthic biomass in hadal trenches: a modelling approach
934 to investigate the effect of vertical and lateral organic matter transport to the seafloor, *Deep Sea Res. Part*
935 *Oceanogr. Res. Pap.*, 100, 21–33, 2015.

936 Imhoff, J. F.: Taxonomy and physiology of phototrophic purple bacteria and green sulfur bacteria, in: *Anoxygenic*
937 *photosynthetic bacteria*, Springer, 1–15, 1995.

- 938 Inthorn, M., Wagner, T., Scheeder, G., and Zabel, M.: Lateral transport controls distribution, quality, and burial
939 of organic matter along continental slopes in high-productivity areas, *Geology*, 34, 205–208, 2006.
- 940 Itoh, M., Kawamura, K., Kitahashi, T., Kojima, S., Katagiri, H., and Shimanaga, M.: Bathymetric patterns of
941 meiofaunal abundance and biomass associated with the Kuril and Ryukyu trenches, western North Pacific Ocean,
942 *Deep Sea Res. Part Oceanogr. Res. Pap.*, 58, 86–97, 2011.
- 943 Itou, M., Matsumura, I., and Noriki, S.: A large flux of particulate matter in the deep Japan Trench observed just
944 after the 1994 Sanriku-Oki earthquake, *Deep Sea Res. Part Oceanogr. Res. Pap.*, 47, 1987–1998, 2000.
- 945 Jahnke, R. A. and Jahnke, D. B.: Rates of C, N, P and Si recycling and denitrification at the US Mid-Atlantic
946 continental slope depocenter, *Deep Sea Res. Part Oceanogr. Res. Pap.*, 47, 1405–1428, 2000.
- 947 Jahnke, R. A., Reimers, C. E., and Craven, D. B.: Intensification of recycling of organic matter at the sea floor
948 near ocean margins, *Nature*, 348, 50–54, 1990.
- 949 Jamieson, A. J., Fujii, T., Mayor, D. J., Solan, M., and Priede, I. G.: Hadal trenches: the ecology of the deepest
950 places on Earth, *Trends Ecol. Evol.*, 25, 190–197, 2010.
- 951 Jebbar, M., Franzetti, B., Girard, E., and Oger, P.: Microbial diversity and adaptation to high hydrostatic pressure
952 in deep-sea hydrothermal vents prokaryotes, *Extremophiles*, 19, 721–740, 2015.
- 953
- 954 Kalisch, B., Dörmann, P., and Hölzl, G.: DGDG and glycolipids in plants and algae, *Lipids Plant Algae Dev.*, 51–
955 83, 2016.
- 956 Kaneda, T.: Iso-and anteiso-fatty acids in bacteria: biosynthesis, function, and taxonomic significance., *Microbiol.*
957 *Mol. Biol. Rev.*, 55, 288–302, 1991.
- 958 Kato, C., Masui, N., and Horikoshi, K.: Properties of obligately barophilic bacteria isolated from a sample of
959 deep-sea sediment from the Izu-Bonin trench, *Oceanogr. Lit. Rev.*, 1, 53–54, 1997.
- 960 Kato, M., Adachi, K., Hagiuro-Nakanishi, K., Ishigaki, E., Sano, H., and Miyachi, S.: betaine lipid from *Pavlova*
961 *lutheri*, *Phytochemistry*, 1994.
- 962 Kioka, A., Schwestermann, T., Moernaut, J., Ikehara, K., Kanamatsu, T., Eglinton, T. I., and Strasser, M.: Event
963 stratigraphy in a hadal oceanic trench: The Japan trench as sedimentary archive recording recurrent giant
964 subduction zone earthquakes and their role in organic carbon export to the deep sea, *Front. Earth Sci.*, 7, 319,
965 2019.
- 966 Koblížek, M., Falkowski, P. G., and Kolber, Z. S.: Diversity and distribution of photosynthetic bacteria in the
967 Black Sea, *Deep Sea Res. Part II Top. Stud. Oceanogr.*, 53, 1934–1944, 2006.
- 968 Koga, Y. and Morii, H.: Biosynthesis of ether-type polar lipids in archaea and evolutionary considerations,
969 *Microbiol. Mol. Biol. Rev.*, 71, 97–120, 2007.

- 970 Komatsu, H. and Chong, P. L.-G.: Low permeability of liposomal membranes composed of bipolar tetraether
971 lipids from thermoacidophilic archaeobacterium *Sulfolobus acidocaldarius*, *Biochemistry*, 37, 107–115, 1998.
- 972 Lam, P., Jensen, M. M., Lavik, G., McGinnis, D. F., Müller, B., Schubert, C. J., Amann, R., Thamdrup, B., and
973 Kuypers, M. M.: Linking crenarchaeal and bacterial nitrification to anammox in the Black Sea, *Proc. Natl. Acad.*
974 *Sci.*, 104, 7104–7109, 2007.
- 975 Lechevalier, H.: Chemotaxonomic use of lipids-an overview, *Microb. Lipids*, 1, 869–902, 1988.
- 976 Leduc, D., Rowden, A. A., Glud, R. N., Wenzhöfer, F., Kitazato, H., and Clark, M. R.: Comparison between
977 infaunal communities of the deep floor and edge of the Tonga Trench: possible effects of differences in organic
978 matter supply, *Deep Sea Res. Part Oceanogr. Res. Pap.*, 116, 264–275, 2016.
- 979 Lipp, J. S. and Hinrichs, K.-U.: Structural diversity and fate of intact polar lipids in marine sediments, *Geochim.*
980 *Cosmochim. Acta*, 73, 6816–6833, 2009a.
- 981 Lipp, J. S. and Hinrichs, K.-U.: Structural diversity and fate of intact polar lipids in marine sediments, *Geochim.*
982 *Cosmochim. Acta*, 73, 6816–6833, 2009b.
- 983 Lipp, J. S., Morono, Y., Inagaki, F., and Hinrichs, K.-U.: Significant contribution of Archaea to extant biomass in
984 marine subsurface sediments, *Nature*, 454, 991–994, 2008.
- 985 Liu, J., Zheng, Y., Lin, H., Wang, X., Li, M., Liu, Y., Yu, M., Zhao, M., Pedentchouk, N., Lea-Smith, D. J., and
986 others: Proliferation of hydrocarbon-degrading microbes at the bottom of the Mariana Trench, *Microbiome*, 7, 1–
987 13, 2019.
- 988 Liu, X., Lipp, J. S., and Hinrichs, K.-U.: Distribution of intact and core GDGTs in marine sediments, *Org.*
989 *Geochem.*, 42, 368–375, 2011.
- 990 Liu, X.-L., Lipp, J. S., Simpson, J. H., Lin, Y.-S., Summons, R. E., and Hinrichs, K.-U.: Mono-and dihydroxyl
991 glycerol dibiphytanyl glycerol tetraethers in marine sediments: Identification of both core and intact polar lipid
992 forms, *Geochim. Cosmochim. Acta*, 89, 102–115, 2012.
- 993 Logemann, J., Graue, J., Köster, J., Engelen, B., Rullkötter, J., and Cypionka, H.: A laboratory experiment of
994 intact polar lipid degradation in sandy sediments, *Biogeosciences*, 8, 2547–2560, 2011.
- 995 López-Lara, I. M., Sohlenkamp, C., and Geiger, O.: Membrane lipids in plant-associated bacteria: their
996 biosyntheses and possible functions, *Mol. Plant. Microbe Interact.*, 16, 567–579, 2003.
- 997 Lund, E. D. and Chu, F.-L. E.: Phospholipid biosynthesis in the oyster protozoan parasite, *Perkinsus marinus*,
998 *Mol. Biochem. Parasitol.*, 121, 245–253, 2002.
- 999 Luo, M., Gieskes, J., Chen, L., Shi, X., and Chen, D.: Provenances, distribution, and accumulation of organic
1000 matter in the southern Mariana Trench rim and slope: Implication for carbon cycle and burial in hadal trenches,
1001 *Mar. Geol.*, 386, 98–106, 2017.

- 1002 Macdonald, A.: The effects of pressure on the molecular structure and physiological functions of cell membranes,
1003 Philos. Trans. R. Soc. Lond. B Biol. Sci., 304, 47–68, 1984.
- 1004 Makula, R.: Phospholipid composition of methane-utilizing bacteria., J. Bacteriol., 134, 771–777, 1978.
- 1005 Mangelsdorf, K., Zink, K.-G., Birrien, J.-L., and Toffin, L.: A quantitative assessment of pressure dependent
1006 adaptive changes in the membrane lipids of a piezosensitive deep sub-seafloor bacterium, Org. Geochem., 36,
1007 1459–1479, 2005.
- 1008 Martin, J. H., Knauer, G. A., Karl, D. M., and Broenkow, W. W.: VERTEX: carbon cycling in the northeast
1009 Pacific, Deep Sea Res. Part Oceanogr. Res. Pap., 34, 267–285, 1987.
- 1010 Matys, E., Sepúlveda, J., Pantoja, S., Lange, C., Caniupán, M., Lamy, F., and Summons, R. E.:
1011 Bacteriohopanepolyols along redox gradients in the Humboldt Current System off northern Chile, Geobiology,
1012 15, 844–857, 2017.
- 1013 Mayzaud, P., Virtue, P., and Albessard, E.: Seasonal variations in the lipid and fatty acid composition of the
1014 euphausiid *Meganyctiphanes norvegica* from the Ligurian Sea, Mar. Ecol. Prog. Ser., 186, 199–210, 1999.
- 1015 Mirzaei, A., Rahmati, M., and Ahmadi, M.: A new method for hierarchical clustering combination, Intell. Data
1016 Anal., 12, 549–571, 2008.
- 1017 Murata, N. and Siegenthaler, P.-A.: Lipids in photosynthesis: an overview, Lipids Photosynth. Struct. Funct.
1018 Genet., 1–20, 1998.
- 1019 Morii, H., Ogawa, M., Fukuda, K. and Taniguchi, H. Ubiquitous distribution of phosphatidylinositol phosphate
1020 synthase and archaetidylinositol phosphate synthase in Bacteria and Archaea, which contain inositol phospholipid,
1021 Biochem. Bioph. Res, 275, 36568–36574, 2014.
- 1022 Nichols, D. S., Miller, M. R., Davies, N. W., Goodchild, A., Raftery, M., and Cavicchioli, R.: Cold adaptation in
1023 the Antarctic archaeon *Methanococcoides burtonii* involves membrane lipid unsaturation, J. Bacteriol., 186,
1024 8508–8515, 2004.
- 1025 Nunoura, T., Takaki, Y., Hirai, M., Shimamura, S., Makabe, A., Koide, O., Kikuchi, T., Miyazaki, J., Koba, K.,
1026 Yoshida, N., and others: Hadal biosphere: insight into the microbial ecosystem in the deepest ocean on Earth,
1027 Proc. Natl. Acad. Sci., 112, E1230–E1236, 2015.
- 1028 Nunoura, T., Hirai, M., Yoshida-Takashima, Y., Nishizawa, M., Kawagucci, S., Yokokawa, T., Miyazaki, J.,
1029 Koide, O., Makita, H., Takaki, Y., and others: Distribution and niche separation of planktonic microbial
1030 communities in the water columns from the surface to the hadal waters of the Japan Trench under the Eutrophic
1031 Ocean, Front. Microbiol., 7, 1261, 2016.
- 1032 Nunoura, T., Nishizawa, M., Hirai, M., Shimamura, S., Harnvoravongchai P., Koide, O., Morono, Y., Fukui, T.,
1033 Inagaki, F., Miyazaki, J., Takaki, Y., and others: Microbial Diversity in Sediments from the Bottom of the
1034 Challenger Deep, the Mariana Trench, Microbes Environ, 33, 186–194, 2018.

- 1035 Oksanen, J., Blanchet, F. G., Kindt, R., Legendre, P., Minchin, P., O'hara, R., Simpson, G., Solymos, P., Stevens,
1036 M., Wagner, H., and others: Community ecology package, R Package Version, 2, 2013.
- 1037 Oliver, J. D. and Colwell, R. R.: Extractable lipids of gram-negative marine bacteria: phospholipid composition,
1038 J. Bacteriol., 114, 897–908, 1973.
- 1039 Patton, S., Lee, R. F., and Benson, A. A.: The presence of unusually high levels of lysophosphatidylethanolamine
1040 in a wax ester-synthesizing copepod (*Calanus plumchrus*), Biochim. Biophys. Acta BBA-Lipids Lipid Metab.,
1041 270, 479–488, 1972.
- 1042 Periasamy, N., Teichert, H., Weise, K., Vogel, R. F., and Winter, R.: Effects of temperature and pressure on the
1043 lateral organization of model membranes with functionally reconstituted multidrug transporter LmrA, Biochim.
1044 Biophys. Acta BBA-Biomembr., 1788, 390–401, 2009.
- 1045
- 1046 Petersen, S. O., Henriksen, K., Blackburn, T. H., and King, G. M.: A comparison of phospholipid and chloroform
1047 fumigation analyses for biomass in soil: potentials and limitations, FEMS Microbiol. Lett., 85, 257–267, 1991.
- 1048 Pitcher, A. M.: Intact polar lipids of ammonia-oxidizing Archaea: structural diversity application in molecular
1049 ecology, PhD Thesis, Departement Aardwetenschappen, 2011.
- 1050 Poff, K. E., Leu, A. O., Eppley, J. M., Karl, D. M., and DeLong, E. F.: Microbial dynamics of elevated carbon
1051 flux in the open ocean's abyss, Proc. Natl. Acad. Sci., 118, 2021.
- 1052 Pond, D. and Harris, R.: The lipid composition of the coccolithophore *Emiliana huxleyi* and its possible
1053 ecophysiological significance, J. Mar. Biol. Assoc. U. K., 76, 579–594, 1996.
- 1054 Popendorf, K., Tanaka, T., Pujo-Pay, M., Lagaria, A., Courties, C., Conan, P., Oriol, L., Sofen, L., Moutin, T.,
1055 and Van Mooy, B. A.: Gradients in intact polar diacylglycerolipids across the Mediterranean Sea are related to
1056 phosphate availability, Biogeosciences, 8, 3733–3745, 2011a.
- 1057 Popendorf, K. J., Lomas, M. W., and Van Mooy, B. A.: Microbial sources of intact polar diacylglycerolipids in
1058 the Western North Atlantic Ocean, Org. Geochem., 42, 803–811, 2011b.
- 1059 Ratledge, C. and Wilkinson, S. G.: Microbial lipids, Academic press, 1988.
- 1060 Rex, M. A., Etter, R. J., Morris, J. S., Crouse, J., McClain, C. R., Johnson, N. A., Stuart, C. T., Deming, J. W.,
1061 Thies, R., and Avery, R.: Global bathymetric patterns of standing stock and body size in the deep-sea benthos,
1062 Mar. Ecol. Prog. Ser., 317, 1–8, 2006.
- 1063 Řezanka, T. and Sigler, K.: Odd-numbered very-long-chain fatty acids from the microbial, animal and plant
1064 kingdoms, Prog. Lipid Res., 48, 206–238, 2009.
- 1065 Řezanka, T., Viden, I., Go, J., Dor, I., and Dembitsky, V.: Polar lipids and fatty acids of three wild cyanobacterial
1066 strains of the genus *Chroococcidiopsis*, Folia Microbiol. (Praha), 48, 781–786, 2003.

- 1067 Rossel, P. E., Elvert, M., Ramette, A., Boetius, A., and Hinrichs, K.-U.: Factors controlling the distribution of
1068 anaerobic methanotrophic communities in marine environments: evidence from intact polar membrane lipids,
1069 *Geochim. Cosmochim. Acta*, 75, 164–184, 2011.
- 1070 Rütters, H., Sass, H., Cypionka, H., and Rullkötter, J.: Monoalkylether phospholipids in the sulfate-reducing
1071 bacteria *Desulfosarcina variabilis* and *Desulforhabdus amnigenus*, *Arch. Microbiol.*, 176, 435–442, 2001.
- 1072 Sabbatini, A., Morigi, C., Negri, A., and Gooday, A. J.: Soft-shelled benthic foraminifera from a hadal site (7800
1073 m water depth) in the Atacama Trench (SE Pacific): preliminary observations, *J. Micropalaeontology*, 21, 131–
1074 135, 2002.
- 1075 Sakurai, I., Shen, J.-R., Leng, J., Ohashi, S., Kobayashi, M., and Wada, H.: Lipids in oxygen-evolving
1076 photosystem II complexes of cyanobacteria and higher plants, *J. Biochem. (Tokyo)*, 140, 201–209, 2006.
- 1077 Sato, N.: Betaine lipids, *Bot. Mag. Shokubutsu-Gaku-Zasshi*, 105, 185–197, 1992.
- 1078 Sato, N., Hagio, M., Wada, H., and Tsuzuki, M.: Requirement of phosphatidylglycerol for photosynthetic function
1079 in thylakoid membranes, *Proc. Natl. Acad. Sci.*, 97, 10655–10660, 2000.
- 1080 Schauburger, C., Middelboe, M., Larsen, M., Peoples, L. M., Bartlett, D. H., Kirpekar, F., Rowden, A. A.,
1081 Wenzhöfer, F., Thamdrup, B., and Glud, R. N.: Spatial variability of prokaryotic and viral abundances in the
1082 Kermadec and Atacama Trench regions, *Limnol. Oceanogr.*, 2021.
- 1083 Schneider, W., Fuenzalida, R., Garcés-Vargas, J., Bravo, L., and Lange, C.: Extensión vertical y horizontal de la
1084 zona de mínima oxígeno en el Pacífico Sur Oriental, *Gayana Concepc.*, 70, 79–82, 2006.
- 1085 Schouten, S., Middelburg, J. J., Hopmans, E. C., and Damsté, J. S. S.: Fossilization and degradation of intact polar
1086 lipids in deep subsurface sediments: a theoretical approach, *Geochim. Cosmochim. Acta*, 74, 3806–3814, 2010.
- 1087 Schubotz, F., Wakeham, S. G., Lipp, J. S., Fredricks, H. F., and Hinrichs, K.-U.: Detection of microbial biomass
1088 by intact polar membrane lipid analysis in the water column and surface sediments of the Black Sea, *Environ.*
1089 *Microbiol.*, 11, 2720–2734, 2009a.
- 1090 Schubotz, F., Wakeham, S. G., Lipp, J. S., Fredricks, H. F., and Hinrichs, K.-U.: Detection of microbial biomass
1091 by intact polar membrane lipid analysis in the water column and surface sediments of the Black Sea, *Environ.*
1092 *Microbiol.*, 11, 2720–2734, 2009b.
- 1093 Schubotz, F., Meyer-Dombard, D., Bradley, A. S., Fredricks, H. F., Hinrichs, K.-U., Shock, E., and Summons, R.
1094 E.: Spatial and temporal variability of biomarkers and microbial diversity reveal metabolic and community
1095 flexibility in Streamer Biofilm Communities in the Lower Geyser Basin, Yellowstone National Park, *Geobiology*,
1096 11, 549–569, 2013.
- 1097 Schubotz, F., Xie, S., Lipp, J. S., Hinrichs, K.-U., and Wakeham, S. G.: Intact polar lipids in the water column of
1098 the eastern tropical North Pacific: abundance and structural variety of non-phosphorus lipids, *Biogeosciences*, 15,
1099 6481–6501, 2018a.

- 1100 Schwestermann, T., Eglinton, T., Haghipour, N., McNichol, A., Ikehara, K., and Strasser, M.: Event-dominated
1101 transport, provenance, and burial of organic carbon in the Japan Trench, *Earth Planet. Sci. Lett.*, 563, 116870,
1102 2021.
- 1103 Sebastián, M., Smith, A. F., González, J. M., Fredricks, H. F., Van Mooy, B., Koblížek, M., Brandsma, J., Koster,
1104 G., Mestre, M., Mostajir, B., and others: Lipid remodelling is a widespread strategy in marine heterotrophic
1105 bacteria upon phosphorus deficiency, *ISME J.*, 10, 968–978, 2016.
- 1106 Shaw, N.: Lipid composition as a guide to the classification of bacteria, *Adv. Appl. Microbiol.*, 17, 63–108, 1974.
- 1107 Siegenthaler, P.-A.: Molecular organization of acyl lipids in photosynthetic membranes of higher plants, in: *Lipids*
1108 in photosynthesis: structure, function and genetics, Springer, 119–144, 1998.
- 1109 Siliakus, M. F., van der Oost, J., and Kengen, S. W.: Adaptations of archaeal and bacterial membranes to variations
1110 in temperature, pH and pressure, *Extremophiles*, 21, 651–670, 2017.
- 1111 Smith, C.: Chemosynthesis in the deep-sea: life without the sun, *Biogeosciences Discuss.*, 9, 17037–17052, 2012.
- 1112 Sohlenkamp, C., López-Lara, I. M., and Geiger, O.: Biosynthesis of phosphatidylcholine in bacteria, *Prog. Lipid*
1113 *Res.*, 42, 115–162, 2003.
- 1114 Somero, G. N.: Adaptations to high hydrostatic pressure., *Annu. Rev. Physiol.*, 54, 557–577, 1992.
- 1115 Stockton, W. L. and DeLaca, T. E.: Food falls in the deep sea: occurrence, quality, and significance, *Deep Sea*
1116 *Res. Part Oceanogr. Res. Pap.*, 29, 157–169, 1982.
- 1117 Sturt, H. F., Summons, R. E., Smith, K., Elvert, M., and Hinrichs, K.-U.: Intact polar membrane lipids in
1118 prokaryotes and sediments deciphered by high-performance liquid chromatography/electrospray ionization
1119 multistage mass spectrometry—new biomarkers for biogeochemistry and microbial ecology, *Rapid Commun.*
1120 *Mass Spectrom.*, 18, 617–628, 2004.
- 1121 Suzuki, R. and Shimodaira, H.: Pvcclust: an R package for assessing the uncertainty in hierarchical clustering,
1122 *Bioinformatics*, 22, 1540–1542, 2006.
- 1123 Ta, K., Peng, X., Xu, H., Du, M., Chen, S., Li, J., and Zhang, C.: Distributions and sources of glycerol dialkyl
1124 glycerol tetraethers in sediment cores from the Mariana subduction zone, *J. Geophys. Res. Biogeosciences*, 124,
1125 857–869, 2019.
- 1126 Tamburini, C., Boutrif, M., Garel, M., Colwell, R. R., and Deming, J. W.: Prokaryotic responses to hydrostatic
1127 pressure in the ocean—a review, *Environ. Microbiol.*, 15, 1262–1274, 2013.
- 1128 Tarn, J., Peoples, L. M., Hardy, K., Cameron, J., and Bartlett, D. H.: Identification of free-living and particle-
1129 associated microbial communities present in hadal regions of the Mariana Trench, *Front. Microbiol.*, 7, 665, 2016.

- 1130 Thompson Jr, G. A.: Lipids and membrane function in green algae, *Biochim. Biophys. Acta BBA-Lipids Lipid*
1131 *Metab.*, 1302, 17–45, 1996.
- 1132 Turnewitsch, R., Falahat, S., Stehlikova, J., Oguri, K., Glud, R. N., Middelboe, M., Kitazato, H., Wenzhöfer, F.,
1133 Ando, K., Fujio, S., and others: Recent sediment dynamics in hadal trenches: evidence for the influence of higher-
1134 frequency (tidal, near-inertial) fluid dynamics, *Deep Sea Res. Part Oceanogr. Res. Pap.*, 90, 125–138, 2014.
- 1135 Van Mooy, B. A. and Fredricks, H. F.: Bacterial and eukaryotic intact polar lipids in the eastern subtropical South
1136 Pacific: water-column distribution, planktonic sources, and fatty acid composition, *Geochim. Cosmochim. Acta*,
1137 74, 6499–6516, 2010.
- 1138 Van Mooy, B. A., Rocap, G., Fredricks, H. F., Evans, C. T., and Devol, A. H.: Sulfolipids dramatically decrease
1139 phosphorus demand by picocyanobacteria in oligotrophic marine environments, *Proc. Natl. Acad. Sci.*, 103, 8607–
1140 8612, 2006.
- 1141 Van Mooy, B. A., Fredricks, H. F., Pedler, B. E., Dyhrman, S. T., Karl, D. M., Koblížek, M., Lomas, M. W.,
1142 Mincer, T. J., Moore, L. R., Moutin, T., and others: Phytoplankton in the ocean use non-phosphorus lipids in
1143 response to phosphorus scarcity, *Nature*, 458, 69–72, 2009.
- 1144 Vardi, A., Van Mooy, B. A., Fredricks, H. F., Pependorf, K. J., Ossolinski, J. E., Haramaty, L., and Bidle, K. D.:
1145 Viral glycosphingolipids induce lytic infection and cell death in marine phytoplankton, *Science*, 326, 861–865,
1146 2009.
- 1147 Vargas, C. A., Cantarero, S. I., Sepúlveda, J., Galán, A., De Pol-Holz, R., Walker, B., Schneider, W., Farías, L.,
1148 D’Ottone, M. C., Walker, J., and others: A source of isotopically light organic carbon in a low-pH anoxic marine
1149 zone, *Nat. Commun.*, 12, 1–11, 2021.
- 1150 Volkman, J., Jeffrey, S., Nichols, P., Rogers, G., and Garland, C.: Fatty acid and lipid composition of 10 species
1151 of microalgae used in mariculture, *J. Exp. Mar. Biol. Ecol.*, 128, 219–240, 1989.
- 1152 Wada, H. and Murata, N.: Membrane lipids in cyanobacteria, in: *Lipids in photosynthesis: structure, function and*
1153 *genetics*, Springer, 65–81, 1998.
- 1154 Wada, H. and Murata, N.: The essential role of phosphatidylglycerol in photosynthesis, *Photosynth. Res.*, 92,
1155 205–215, 2007.
- 1156 Wakeham, S. G., Lee, C., Farrington, J. W., and Gagosian, R. B.: Biogeochemistry of particulate organic matter
1157 in the oceans: results from sediment trap experiments, *Deep Sea Res. Part Oceanogr. Res. Pap.*, 31, 509–528,
1158 1984.
- 1159 Wakeham, S. G., Amann, R., Freeman, K. H., Hopmans, E. C., Jørgensen, B. B., Putnam, I. F., Schouten, S.,
1160 Damsté, J. S. S., Talbot, H. M., and Woebken, D.: Microbial ecology of the stratified water column of the Black
1161 Sea as revealed by a comprehensive biomarker study, *Org. Geochem.*, 38, 2070–2097, 2007.

1162 Wakeham, S. G., Turich, C., Schubotz, F., Podlaska, A., Li, X. N., Varela, R., Astor, Y., Saenz, J. P., Rush, D.,
 1163 Damste, J. S. S., and others: Biomarkers, chemistry and microbiology show chemoautotrophy in a multilayer
 1164 chemocline in the Cariaco Basin, *Deep Sea Res. Part Oceanogr. Res. Pap.*, 63, 133–156, 2012.

1165 Warnes, G., Bolker, B., Bonebakker, L., Gentleman, R., Liaw, W., Lumley, T., and others: gplots: various R
 1166 programming tools for plotting data. R package version 2.16. 0. 2015, 2015.

1167 Warton, D. I., Wright, S. T., and Wang, Y.: Distance-based multivariate analyses confound location and dispersion
 1168 effects, *Methods Ecol. Evol.*, 3, 89–101, 2012.

1169 Weijers, J. W., Schouten, S., van den Donker, J. C., Hopmans, E. C., and Damsté, J. S. S.: Environmental controls
 1170 on bacterial tetraether membrane lipid distribution in soils, *Geochim. Cosmochim. Acta*, 71, 703–713, 2007.

1171 Wenzhöfer, F., Oguri, K., Middelboe, M., Turnewitsch, R., Toyofuku, T., Kitazato, H., and Glud, R. N.: Benthic
 1172 carbon mineralization in hadal trenches: Assessment by in situ O₂ microprofile measurements, *Deep Sea Res.*
 1173 *Part Oceanogr. Res. Pap.*, 116, 276–286, 2016.

1174 Wenzhöfer, F. The Expedition SO261 of the Research Vessel SONNE to the Atacama Trench in the Pacific Ocean
 1175 in 2018. *Rep Polar Mar Res* 729:1–111. 2019.

1176 Westrich, J. T. and Berner, R. A.: The role of sedimentary organic matter in bacterial sulphate reduction – the G
 1177 model tested, *Limnol. Oceanogr.*, 29, 236–249, 1984.

1178 White, D., Bobbie, R., King, J., Nickels, J., and Amoe, P.: Lipid analysis of sediments for microbial biomass and
 1179 community structure, in: *Methodology for biomass determinations and microbial activities in sediments*, ASTM
 1180 International, 1979.

1181 Winter, R.: Effect of lipid chain length, temperature, pressure and composition on the lateral organisation and
 1182 phase behavior of lipid bilayer/gramicidin mixtures, in: *Biophysical Journal*, 153A-153A, 2002.

1183 Winter, R. and Jeworrek, C.: Effect of pressure on membranes, *Soft Matter*, 5, 3157–3173, 2009.

1184 Wörmer, L., Lipp, J. S., Schröder, J. M., and Hinrichs, K.-U.: Application of two new LC–ESI–MS methods for
 1185 improved detection of intact polar lipids (IPLs) in environmental samples, *Org. Geochem.*, 59, 10–21, 2013.

1186 Xu, Y., Ge, H., and Fang, J.: Biogeochemistry of hadal trenches: Recent developments and future perspectives,
 1187 *Deep Sea Res. Part II Top. Stud. Oceanogr.*, 155, 19–26, 2018.

1188 Xu, Y., Jia, Z., Xiao, W., Fang, J., Wang, Y., Luo, M., Wenzhöfer, F., Rowden, A. A., and Glud, R. N.: Glycerol
 1189 dialkyl glycerol tetraethers in surface sediments from three Pacific trenches: Distribution, source and
 1190 environmental implications, *Org. Geochem.*, 147, 104079, 2020.

1191 Xu, Y., Li, X., Luo, M., Xiao, W., Fang, J., Rashid, H., Peng, Y., Li, W., Wenzhöfer, F., Rowden, A. A., and
 1192 others: Distribution, Source, and Burial of Sedimentary Organic Carbon in Kermadec and Atacama Trenches, *J.*
 1193 *Geophys. Res. Biogeosciences*, 126, e2020JG006189, 2021.

- 1194 Yano, Y., Nakayama, A., Ishihara, K., and Saito, H.: Adaptive changes in membrane lipids of barophilic bacteria
1195 in response to changes in growth pressure, *Appl. Environ. Microbiol.*, 64, 479–485, 1998.
- 1196 Zhong, H., Lehtovirta-Morley, L., Liu, J., Zheng, Y., Lin, H., Song, D., Todd, J. D., Tian, J., and Zhang, X.-H.:
1197 Novel insights into the Thaumarchaeota in the deepest oceans: their metabolism and potential adaptation
1198 mechanisms, *Microbiome*, 8, 1–16, 2020.
- 1199 Zhukova, N. V.: Variation in microbial biomass and community structure in sediments of Peter the Great Bay
1200 (Sea of Japan/East Sea), as estimated from fatty acid biomarkers, *Ocean Sci. J.*, 40, 34–42, 2005.